Thiobarbituric acid a useful scaffold for medicinal chemistry

2018

Sikabwe Noki

Thiobarbituric acid a useful scaffold for medicinal chemistry

210506519

Sikabwe Noki

2018

This thesis is submitted to the School of Health Sciences, College of Health Science, University of KwaZulu-Natal, Westville, to satisfy the requirements for the degree of Master of Medical Science in Pharmaceutical Chemistry.

This is a thesis in which the chapters are written as a set of discrete research publications, with an overall introduction and summary. Typically, chapter 2 and chapter 3 will have been published in internationally recognized, peer-reviewed journals.

This is to certify that the contents of this thesis are the original research work of Mr. Sikabwe Noki, carried out under our supervision at Peptide Sciences Laboratory and the Catalysis and Peptide Research Unit, University of KwaZulu-Natal, Westville Campus, Durban, South Africa.

As the candidate's supervisor, I have approved this thesis for submission.

Supervisor:

Signed: _____ Name: **Prof. Fernando Albericio,** Date: _____

Co-Supervisor:

Signed: _____ Name: **Prof. Beatriz G. de la Torre,** Date: _____

ABSTRACT

Due to the growth number of infectious diseases, a huge demand of new antimicrobial agents are required. In this regard, Thiobarbituric acid (TBA) moieties were explored. As its name indicates, TBA is the sulfur version of the barbituric acid. The work in barbituric moieties dated long ago in 1864 by Baeyer, when it was reported that these barbituric derivatives can be used as anesthetics, sedative or anticonvulsive agents.

In the present work and taking advantage that TBA structure shows several points where diversity can be introduced, therefore several functionalities were introduced in the TBA analogues and their antimicrobial properties were studied in Gram-positive and Gram-negative bacteria. (Chapter 1)

These are the chemical modifications explored: i) *N*- substitution, where this site can be substituted with a symmetrical substituents; ii) reaction at C-5 position owing to the high acidity of the protons which includes acylation, acetylation, Schiff bases, Knoevenagel condensation thioamide and enamine formation.

The antimicrobial activity screening for the synthesized compounds were against Gram-positive (*S. aureus* and *B. subtilus*) and Gram negative (*E. coli* and *P. aeruginosa*) bacteria. Among all thiobabituric derivatives synthesized, Boc-Phe-TBA showed a promising activity, which confirms that TBA could be an excellent scaffold when combined with *N*-protected amino acids for developing antimicrobial compounds. (Chapter 2)

The characterization of 20 thiobarbituric derivatives was carried out in different spectroscopy techniques such as: Nuclear Magnetic Resonance (NMR), Ultra violet spectroscopy, Infra-Red spectroscopy and single X-ray crystallography. In NMR characterization the acetylation of TBA was the most interesting due to the fact that this type of compound have the tendency of forming Enol and Keto tautomerism. This was proved by NMR and also by theoretical calculation, and the results confirm that the ^{1}H NMR for this compound **(A01)** showed resonance at 17.72 ppm (singlet) for OH. This indicate that the enol form is more stable than the keto form. In UV characterization due to the fact TBA derivatives are not known aromatic and yet they are UV active. Therefore the absorption of few TBA derivatives were study in different solvents hence these showed absorption

at maximum wavelength (λ_{max}) in the range of 322 – 285 nm respectively. For IR characterization, these derivatives (**A01**, **A02**, **A03**, **A04**, **A06**, **A10**, **A12**, **A13**, **A14** and **A17**) were evaluated, and showed absorption stretching frequency of thiocarbonyl (C=S) in three different ranges, 1395–1570 cm^{-1}, 1260– 11420 cm^{-1} and 940 – 1140 cm^{-1}. For X- ray crystallography, crystals of **A01**, **A02**, **A06**, **A13**, **A17** and **A18** were obtained by hot recrystallization from ethanol and the intramolecular H-Bonding formation was observed in all cases, intermolecular H-bonding was observed for **A17.** (Chapter 3)

DECLARATION I

Plagiarism declaration

I, **Sikabwe Noki** declare that

1. The research work reported in this thesis, except where otherwise indicated, is my original research.
2. This thesis has not been submitted for any degree or examination at any other university.
3. This thesis does not contain other person's data, pictures, graphs or other information, unless specifically acknowledged as being sourced from other persons.
4. This thesis does not contain other person's writing, unless specifically acknowledged as being sourced from other researchers. In cases where other written sources have been quoted:
    a. Their words have been re-written but the general information attributed to them has been referenced.
    b. Where their exact words have been used, then their writing has been placed inside quotation marks, and referenced.
5. This thesis does not contain text, graphics or tables copied and pasted from the internet, unless specifically acknowledged, and the source being detailed in the thesis and in the references sections.

Signed

_____

Sikabwe Noki

DECLARATION II

Publications

List of Publications

Publications part of the thesis

1. **Exploiting the Thiobarbituric Acid Scaffold for Antibacterial Activity (Chapter 2)**
   Anamika Sharma, Sikabwe Noki, Sizwe J. Zamisa, Heba A. Hazzah, Zainab M. Almarhoon, Ayman El-Faham, Beatriz G. de la Torre, Fernando Albericio
   Published article:
   ChemMedChem Peer-reviewed Journal.
   DOI: 10.1002/cmdc.201800414.

   Sikabwe Noki contributed to the synthesis of thiobarbituric derivatives, characterized them using the appropriate techniques, and contributed in the write up of the manuscript.

   Anamika Sharma contributed to the design of the project, synthesized some of the thiobarbituric derivatives, characterized them using the appropriate techniques, and contributed in the write up of the manuscript.

   All the remaining are supervisors

2. **Crystal Structure, Spectroscopic and Theoretical studies of Thiobarbituric Acid Derivatives: Understanding H-Bonding Pattern. (Chapter 3)**
   Anamika Sharma, Sizwe Zamisa, Sikabwe Noki, Zainab M.Almarhoon, Ayman El-Faham, Beatriz G.de la Torre and Fernando Albericio.
   Published article
   Acta Crystallographica Section C Peer-reviewed Journal.
   https://doi.org/10.1107/S2053229618015516

   Sikabwe Noki contributed to the synthesis of thiobarbituric derivatives, characterized them using the appropriate techniques, and contributed in the write up of the manuscript.

Anamika Sharma contributed to the design of the project, synthesized some of the thiobarbituric derivatives, characterized them using the appropriate techniques, and contributed in the write up of the manuscript.

Sizwe Zamisa Contributed to the analysis and characterization of Crystalized Thiobarbituric derivatives using XRD crystallography instrument and contributed in the write up of the manuscript.

All the remaining are supervisors

Other publication

Investigation of the N-Terminus Amino Function of Arg_{10}-Teixobactin

Shimaa .A.H.Abdel Monaim, Sikabwe Noki, Estelle J.Ramchuran, Ayman El-Faham, Fernando Albericio, and Beatriz G.de la Torre.

Published article

Molecules MDPI Journal

DOI: 10.3390/molecules22101632

ACKNOWLEDGMENTS

I would like to direct my heartfelt gratitude to:

- My GOD Almighty for giving me courage, strength, knowledge, capability and to take on this research study, to persevere and complete it successfully, through his blessing lied this achievement.
- My family (Noki family), my mother (**Ndorere Miriam**), my sisters (Rebecca, Salima, Assa, Antoinette, Agrippina, Agade) and brothers (Diouf Beni Baranyizigiye, Felicien, Benjamin).
- My Supervisors, Prof Fernando **Albericio** and Prof **Beatriz de la Torre** for their teaching and guidance throughout the research journey, and for their support throughout the project and the thesis writing. Thank you again for allowing me to be part of the peptides family.
- My mentor, Dr. **Anamika Sharma** for the training and transfer of her knowledge of chemistry to me, my gratitude come from my heart.
- Dr. Yahya Jad, Dr. Shimaa Amin, the Peptides sciences laboratory group, along with the Catalysis and Peptides Research Unit group, for their support throughout this project. They made a huge contribution to my study and life.

Abbreviations

ACN	**:**	Acetonitrile
BA	**:**	Barbituric acid
BOC	**:**	tert-Butyloxycarbonyl
CNS	**:**	Central Nervous System
DCM	**:**	Dichloromethane
DETBA	**:**	1,2 Diethyl thiobabituric acid
DFT	**:**	Density Functional Theory
DMAP	**:**	4-Dimethylaminopyridine
DIEA	**:**	N,N-Diisopropylethylamine
EDC	**:**	1-Ethyl-3-(3-Dimethylaminopropyl) Carbodiimide
EtOH	**:**	Ethanol
FTIR	**:**	Fourier Transform Infrared Spectroscopy
GABA	**:**	Gamma-Aminobutyric acid
H_2SO_4	**:**	Sulfuric acid
HCl	**:**	Hydrochloric Acid
HOBt	**:**	Hydroxybenzotriazole
HOMO	**:**	Highest Occupied Molecular Orbital
HPLC	**:**	High-Performance Liquid Chromatography
HRMS	**:**	High Resolution Mass Spectroscopy
LUMO	**:**	Lowest Unoccupied Molecular Orbital
MIC	**:**	Minimum inhibitory Concentration
NaHCO3	**:**	Sodium hydrogen carbonate
NH4Cl	**:**	Ammonium Chloride
RMSD	**:**	Room mean square deviation
TBA	**:**	Thiobarbituric Acid
TFA	**:**	Trifluoroacetic acid
^{1}H NMR	**:**	Proton Nuclear Magnetic Resonance
^{13}C NMR	**:**	Carbon Nuclear Magnetic Resonance
λmax	**:**	Maximum wavelength

TABLE OF CONTENTS

CHAPTER 1

Introduction

1. Antimicrobial agents and the need for new drugs

A large demand for the development of new antimicrobial agents is still one of the major concern of medicinal chemists. This is due to the increasing number of infectious diseases that affect populations worldwide and in addition, the increase in the number of multi-drug-resistant bacteria, pose a serious threat to human health, therefore the incorporation of new antimicrobial agents will facilitate to fight and cure these infections.[1-2]

The therapy to treat infections caused by bacteria were not advanced in the 1930s and majority of populations suffered from pneumonia, meningitis, typhoid fever, syphilis, tuberculosis, due to the living conditions and the lack of good antimicrobial agents[3] When the antimicrobial agent was developed a new era started to control and treat these diseases.[3] This antimicrobial therapy provided physicians with the ability to combat and cure certain diseases

Our aim was to study the potential of thiobarbituric acid against Gram positive or Gram negative bacteria like *E. coli, S. aureus,* and *P. aeruginosa* .[4]

2. Historical background of barbiturates derivatives.

The barbiturates group contribute enormously in both biological and chemical fields.[5] Although these compounds were officially discovered in 1864, by the German research chemist Baeyer**,** its history had the roots almost one century earlier. Barbituric acid started with the discovery of uric acid by Scheele in 1776[6] and in 1838 Liebig and Wohler oxidized uric acid with nitric acid and formed alloxantin.[7] In 1845 Liebig's student Schlieper synthesized hydurilic acid from uric acid while attempting to make alloxan,[8] followed by oxidized alloxantin to obtain dilituric acid.[9] Baeyer oxidized hydurilic acid to obtain violuric acid which further oxidation yielded dilituric acid. Baeyer investigated these compounds and realized that all these compounds are related and belong to the barbituric acid series.[10] Baeyer heated the mixture of hydurilic acid, nitric acid, and saturated bromine to obtain 5-dibromo barbituric, basically by performing the reaction of bromine

on violuric acid, dilituric acid, or hydurilic acid, obtained alloxanbromide also known as 5-dibromo barbituric acid.[9] He followed by synthesized barbituric acid from 5-dibromo barbituric acid by using two procedures; the first involved heating the reaction of dibromo barbituric acid with sodium amalgam (NaHg) and small amount of water and secondly by reacting dibromo barbituric acid with hydrogen iodide (HI) in water to obtain barbituric acid (first named Malonylurea) as shown in Figure 1.[9]

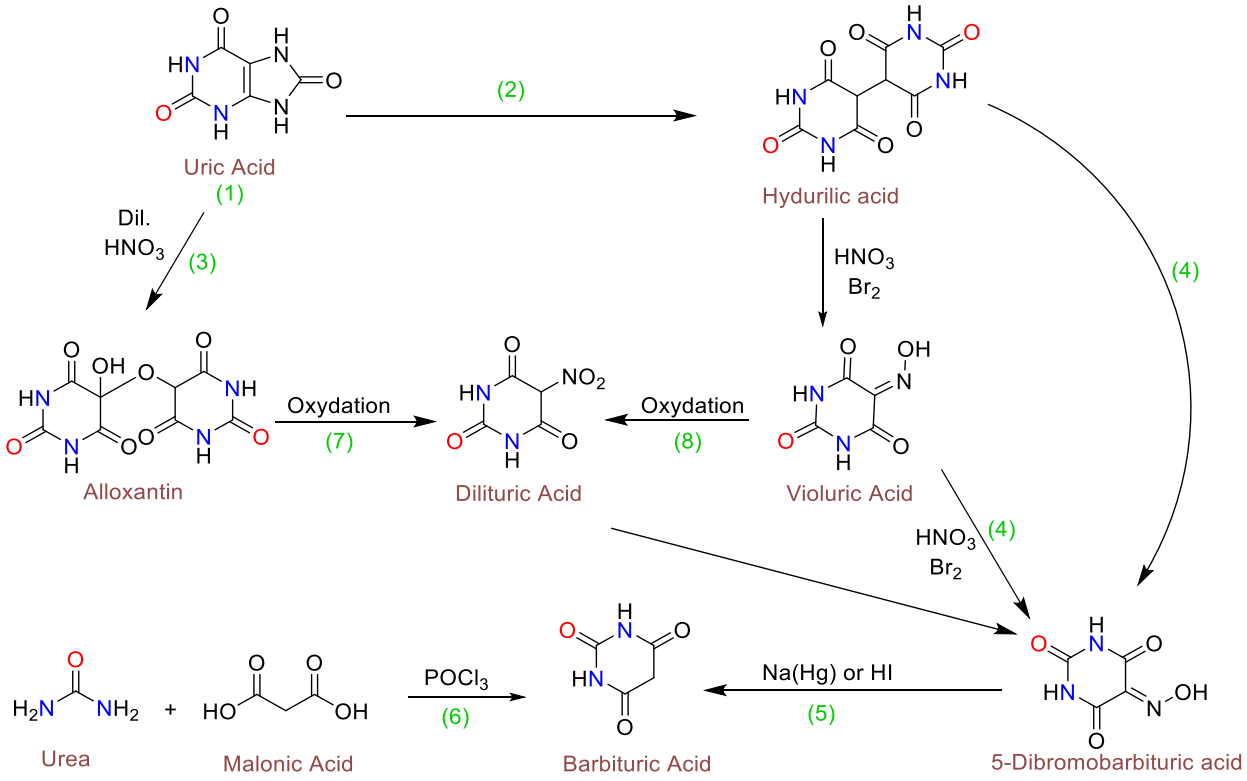

Figure 1: Show the outline of the history of barbituric acid: (1) Schlieper 1845; (2) Sheele 1776 (3) Liebig Wohler 1838; (4) Baeyer 1863; (5) Baeyer 1864; (6) Grimaux 1979; (7) Schlieper; (8) Baeyer.[9]

A few years later Mulder elucidated the correct structure of barbituric acid. Due to Baeyer's procedure for synthesizing barbituric acid was long, subsequently, Grimaux developed in 1879 a straight forward procedure using malonic acid and urea in presence of phosphorous oxychloride, to obtained pure malonylurea (Barbituric acid).[11]

Figure 2 showed general chemical structure of barbiturates, when the X position is substituted with oxygen it's called "Barbiturates (C=O)" and "Thiobarbiturates" if X position is sulfur (C=S).

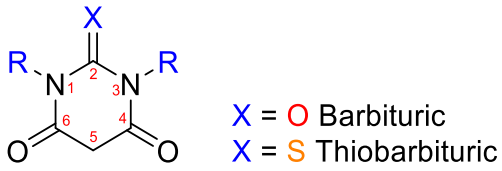

Figure 2: General and numbering of barbiturates

3. The biological significance of (Thio) barbituric acid (TBA/BA)

In 1904, barbiturate was introduced clinically as a sedative-hypnotic agent by the company Farbweke Fr. Bayer .[5] As definition sedative agent decrease tension, anxiety and calm beneficiary whereas a hypnotic agent produces drowsiness and facilitates the start of sleep.[12]

Barbiturates are widely known drugs with activity at the central nervous system (CNS), especially as an anticonvulsant, anxiolytics, tranquilizers and sedatives-hypnotics.[13] According to some literature it has been reported that these drugs inhibit neurotransmitter chemical (acetylcholine, norepinephrine, and glutamate) and the calcium absorption of nerve terminals.[13] The following drugs were among the first barbiturate derivatives (Pentobarbital, Phenobarbital, Amobarbital, Secobarbital,) to show activities at CNS especially as sedative-hypnotics activity (Figure 3).[5]

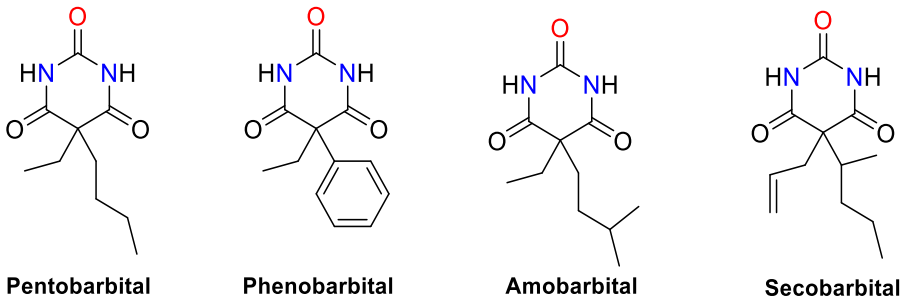

Figure 3: First barbiturate derivatives that showed sedative-hypnotics activities.[5]

Owing to their hypnotic and sedative behavior, nowadays a large number of CNS depressant drugs are available in the market, the most known CNS depressant is Benzodiazepines based which were commercialized in the 1960s.[14]

Although it can be found in the early literature some references to the synthesis of some thio derivatives of the BA structure, the first serious study of the synthesis and biological activity of

thiobarbiturate (TBA) dated back in 1935. Thus, Tabern *et al* in 1935 synthesized TBA analogs and showed to be more active as hypnotics than the oxygen analogs (BA).[15]

Similarly to BAs, TBAs can be used in addition as anesthetics, sedatives or anti-convulsive agents. Its mode of action is through its tendency to bind to specific regions of various receptors e.g. to GABA, nicotinic-acetylcholine (nAChR) or BK channel receptors which are all ligand-gated ion channels.[16] The substituted by alkyl or aryl group at C5 atom increase the binding to the GABA receptors. Furthermore, these substitution increases lipid solubility and simplifies transport of BA and TBA towards their enzyme target.[16]

The discovering of sedative-hypnotic property associated with these type of compounds has fueled the synthesis of thousands of mainly BA and TBA derivatives as well. Modifications explored the substitution of both hydrogen atoms attached to nitrogen and the fifth position present in the BA structure with alkyl and aryl group.[9] These class of compounds rapidly became attractive to a medicinal chemist, as in addition of their original properties,[17-19] they bear a wide range of other biological activities: anti-inflammatory,[20] anti-diabetic,[21] anticonvulsant,[22] anti-HIV,[23] anticancer,[24] antiangiogenic, antihypertensive,[25] antifungal, antibacterial,[26] antimicrobial.[27]

Although there are no commercially drugs based on TBA, these compounds are reported to exhibit better biological potency than BA.[28] This can be due to the presence of the carbon-sulfur bond (C=S).[29] The reason for higher biological activity behavior of TBA derivatives than BA derivatives is due to their better lipid solubility and better hydrogen bond acceptors. This last property simplifies binding to the enzyme receptors. [16] The oxygen and sulfur atoms in C=O and C=S group show differences in their physicochemical and biological properties due to the greater bulk and polarization of the sulfur atom and its decreased electronegativity.[30]

A study on quantitative-structure-activity-relationship (QSAR) of molecules responsible for anesthetic activity reports that electronic factor is more important for biological activity than geometrical factors.[31] The fact that TBA scaffold has not been broadly exploited in term of their biological activity, this gives us an opportunity to explore this core structure for their bioactivity.[32]

4. Antimicrobial activity

Medicinal chemists researched for years to find drugs to substitute the ones that developed bacterial resistance. In literature, the TBA derivatives have been explored for antimicrobial activity associated with structure change at position N1, N3, C2 and C5 (Figure 2).[14]

The target antibacterial potential studies of all synthesis were in Gram-positive and Gram-negative bacteria, particularly *B. cereus, S. aureus, E. Coli, K. pneumonia, P. aeriginosa,* and *S. enterica.*[14] In 2016, Dhorajiya *et al*. reported the MIC values of the chalcones of TBA group and BA group with former showing good potency towards *P. aeruginosa* whereas in case of *E. coli* the chalcones of BA are potent than the chalcones of TBA.[32]

In 2009, Yan *et al*. investigated a series of 5-benzylidene BA and TBA derivatives followed by their evaluation to study inhibitory effects on the diphenolase activity of mushroom tyrosine and their antibacterial activities against Gram-positive and Gram-negative bacteria. The investigation was conducted and the outcome showed that most compounds had potential tyrosinase inhibitory activities, whereby the inhibitory effects of 5-benzylidene TBA on tyrosinase were of similar potency (with an IC_{50} value of 14.49 μM) with 5-benzylidene BA (with an IC_{50} value of 13.98 μM) (Figure 5).

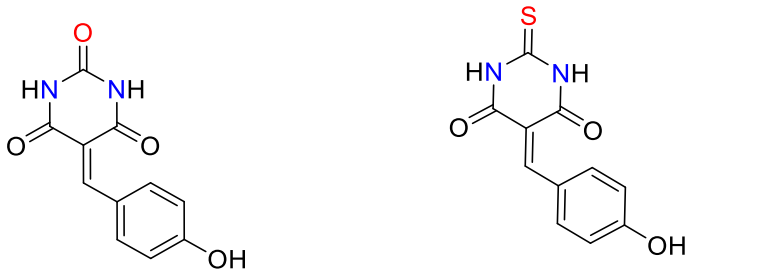

Figure 5: 5-benzylidene BA and 5-benzylidene TBA.

In the case of antibacterial activities, Yan *et al*. reported that all the synthesized 5-benzylidene TBA derivatives showed no antibacterial activities *in vitro* against *S. epidermidis, S. Albus, B. ceres, E. coli,* and *P. aeruginosa*, but comparing 5-benzylidene TBA, **2A**, **2B** and **2C** with 5-benzylidene BA derivatives **1A**, **1B**, and **1C**, this showed thiobarbiturates **2A**, **2B** and **2C** exhibited antimicrobial activities against *S. aureus* with the minimum inhibitory concentration (MIC) value

of 3.1, 3.1 and 6.25 μg/mL respectively, whereas BA derivatives exhibit no antimicrobial activities, supporting the fact that TBA derivatives are more bioactive than BA derivatives.[28]

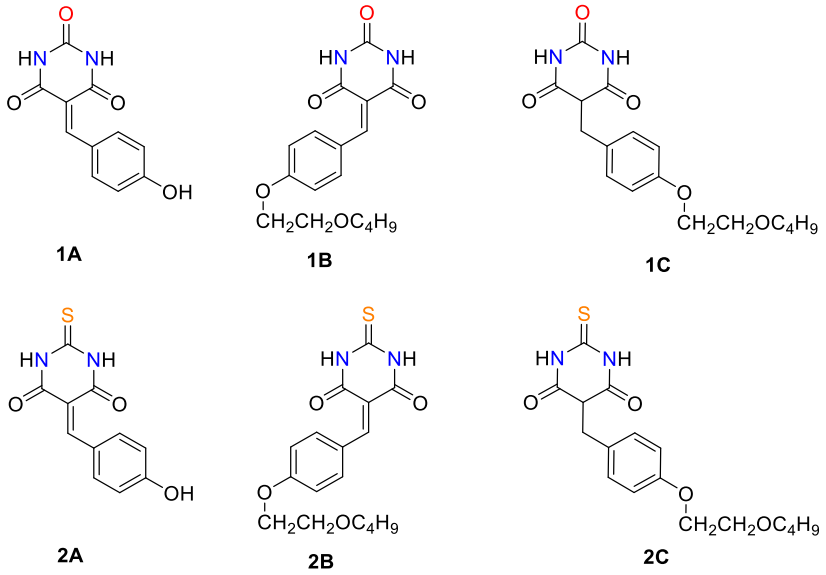

Figure 6: Compared TBA and BA that showed bio-activities against *S.aureus.*

5. Synthesis of thiobarbiturates (TBA) derivatives

As mentioned earlier, several attempts were made to synthesize barbiturates moieties, in 1879, Grimaux developed a straight forward procedure using malonic acid and urea, by mixing them in presence of phosphorous oxychloride to render barbituric acid (Figure 7).[33]

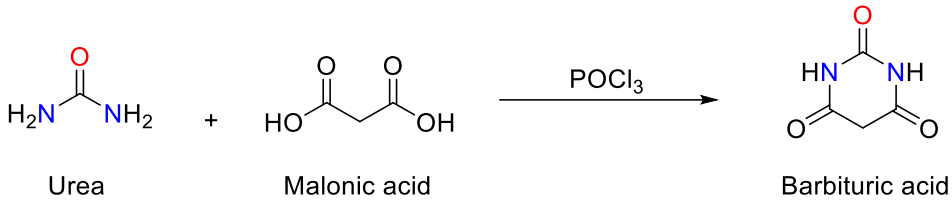

Figure 7: First straight forwards procedure developed for barbituric acid.

A develop an alternative procedure to synthesize (thio)barbituric acid, was conducted using (thio)urea, malonic acid in the presence of acetyl chloride under reflux condition (Figure 8).[34]

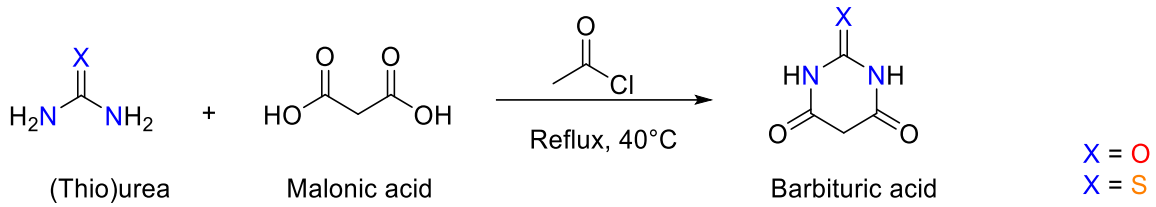

Figure 8: Alternative procedure developed for barbituric acid.

Since the purpose of the project was to explore thiobarbituric acid (TBA) as a scaffold for the development of new antibacterial agents, and there are two sites which can be explored. All the compounds synthesized showed N-substitution to avoid antianxiety properties.[17] In this regard, both "N" were substituted symmetrically, Secondly, C-5 position of TBA structure, since the proton at C-5 position is highly acidic therefore various reactions can be conducted at this position including acylation, acetylation, Schiff bases, Knoevenagel condensation and thioamide reactions, which has been explained below.

5.1. Synthesis of N-Substituted thiobarbituric derivatives.

The synthesis of *N*-substituted TBA derivative is conducted by condensation of an isothiocyanate with the corresponding amine to obtained symmetrical thiourea, follow by reacting the thiourea with malonic acid and acetyl chloride under reflux condition to afford respective *N*-substituted TBA derivative.[34]

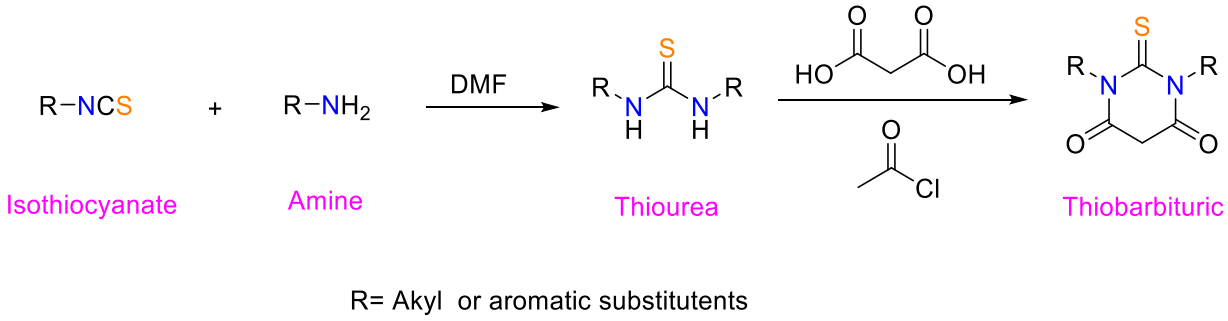

Scheme 1: Synthesis of *N*-substituted thiobarbituric derivatives.

5.2. Schiff base reaction

Schiff bases have been known since the middle of 19th century,[35] since the study started in 1931 with Pfeiff.[36] A Schiff base is formation of imine by a reaction whereby C=O group of an aldehyde or ketone is replaced by carbon-nitrogen double bond (C=N-R_3) group with nitrogen atom connected to an aryl or alkyl group, with a general formula $R_1R_2C{=}NR_3$, where R_3 is preferably a phenyl or alkyl group (leads to stable imine) than an aryl group (leads to unstable imine).[37] The formation of the Schiff base is conducted by condensation of an aldehyde or ketone with a primary amine. The reaction is achieved with a nucleophilic attack of nitrogen from amine towards the carbonyl carbon to give the imine product or Schiff base, it generally takes place under acidic or basic catalyst, Scheme 2.[38]

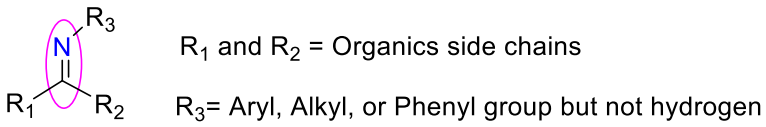

Figure 10: General formula of Schiff base.

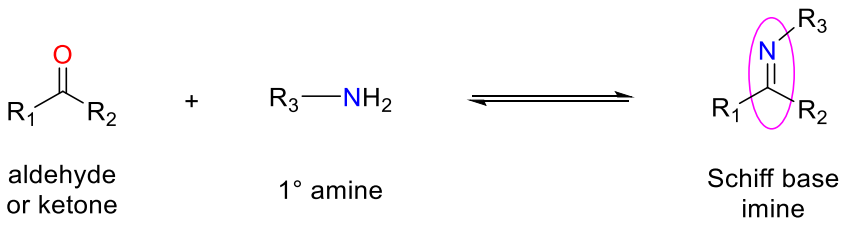

Scheme 2: Synthesis of Schiff base

Schiff bases are widely used as pigment and dyes, catalysts, intermediates in organic synthesis, and as polymer stabilizers,[37] and in addition, they are known for their broad range of biological activities, including antifungal, antibacterial, antimalarial, antiproliferative, anti-inflammatory, antiviral, and antipyretic properties.[39-40] According to literature, in the case of the antibacterial, Schiff bases are known to interact with the lipopolysaccharides present in the outer membrane of bacteria to enhance the membrane permeability of bacteria.[41]

In 2012, Kalaivani, *et al.*, compared the biological activities of Schiff base compounds **A** and **B** (Figure 9) with the standard reference Ciprofloxacin, the results indicate that some of the Schiff bases exhibit microbial activity against *S. epidermis* and *E. coli*.[42]

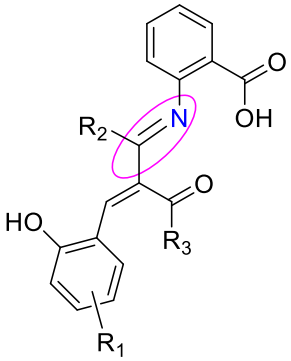

Compound A: R_1 = H, R_2 = C_6H5, R_3 = OC_2H_5

Compound B: R_1 = C_4H4, R_2 = C_6H5, R_3 = OC_2H_5

Figure 9: Schiff base compounds A and B.[42]

Due to the known properties of Schiff bases are as antimicrobials,[37] they could be an excellent platform and therefore Schiff base derivatives of TBA were synthesized.

5.3. Knoevenagel condensation reaction.

Knoevenagel condensation is a reaction between active methylene derivative with a carbonyl compound in presence of base resulting in the formation of an olefin, C=C bond formation, developed in 1890 by Emil Knoevenagel (Scheme 3).[43-45]

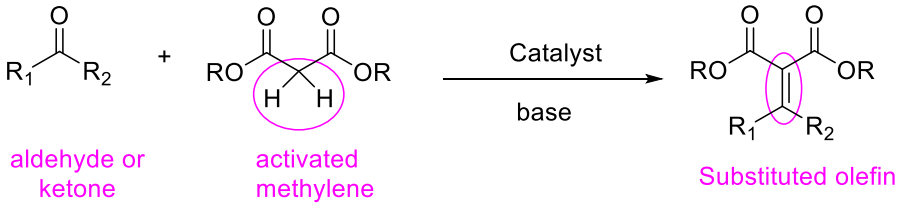

Scheme 3: Knoevenagel condensation reaction

The role of the base is to abstract the acidic proton from the active methylene compound and the most common base used is pyridine, but there are reports where Knoevenagel condensation reaction was carried out in absence of a base. In 2001, Jursic *et al*. reported the Knoevenagel condensation between α, a β-conjugated aldehyde with barbituric acid in methanol (Scheme 4).[29]

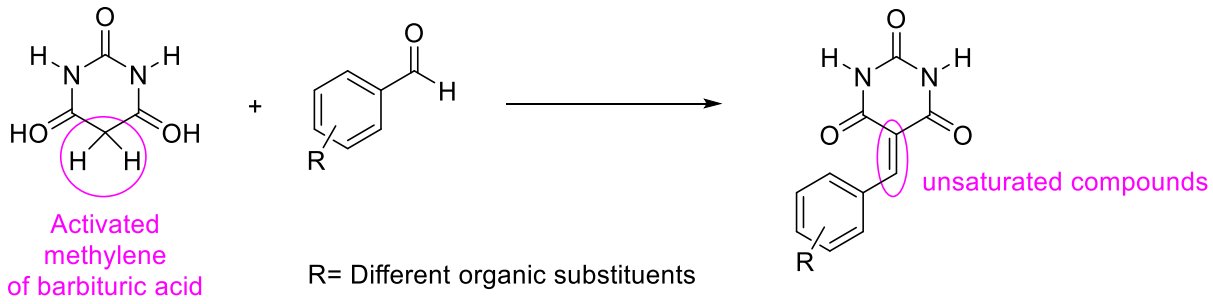

Scheme 4**:** Several products of the Knoevenagel condensation products with barbituric acid as a source of 'active' methylene group.[29]

Due to the presence of the activated methylene compounds,[46] the primary unsaturated product may undergo Michael addition reaction, resulting in bis compounds. Michael addition reaction is a conjugate addition of a carbanion or other nucleophile (Michael donor) to an *α*, *β*-unsaturated carbonyl compound (Michael acceptor) as shown in Figure 10.[47, 46]

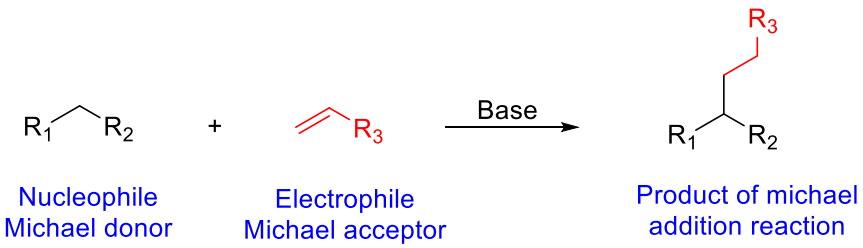

Figure 10: General Michael addition reaction

In Figure 10, the R_1 and R_2 are electron-withdrawing groups (acyl and cyano) increasing the acidic of hydrogen, and R_3 is a ketone (enone), or a nitro group.[48]

The Knoevenagel condensation in case of TBA and aldehyde usually undergo Michael addition depending upon the substituents present on aldehyde.[29, 49, 50] In 1999, Coe *et al*., reported the formation of Michael adduct, when reacted 1,3-diethyl-2-thiobarbituric acid with benzaldehyde derivatives with substituent at *meta, ortho* and *para* position,[49] it was observed that reactivity towards Michael addition increases due to the presence of electron withdrawing substituents (such as –CN, or $–NO_2$) when the molecule becomes more planar.[51]

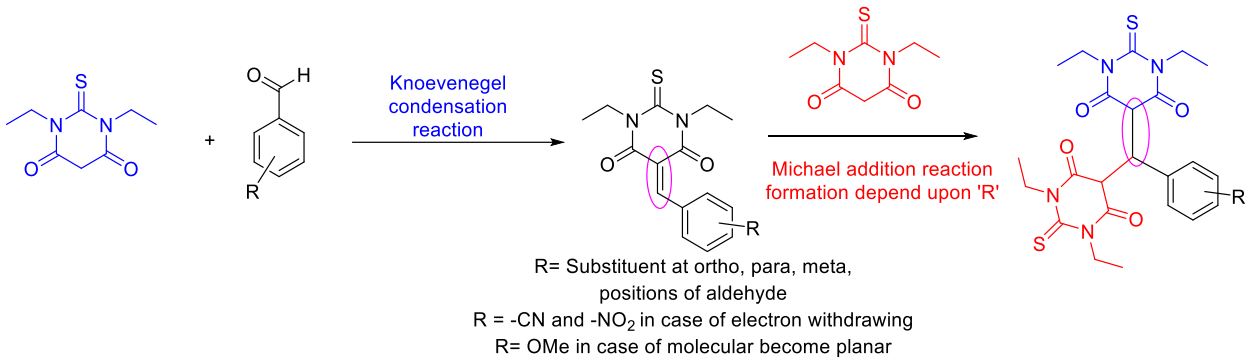

Figure 11: Formation of Michael addition adducts

In 2003, Jursic *et al*., reported whereby a reaction underwent a Michael addition reaction after Knoevenagel condensation reaction, involving a second nucleophilic addition of BA to *α*, *β*-unsaturated carbonyl compounds and this can only be accomplished with the enol form of BA with a strong acid catalyst (Figure 12).[52]

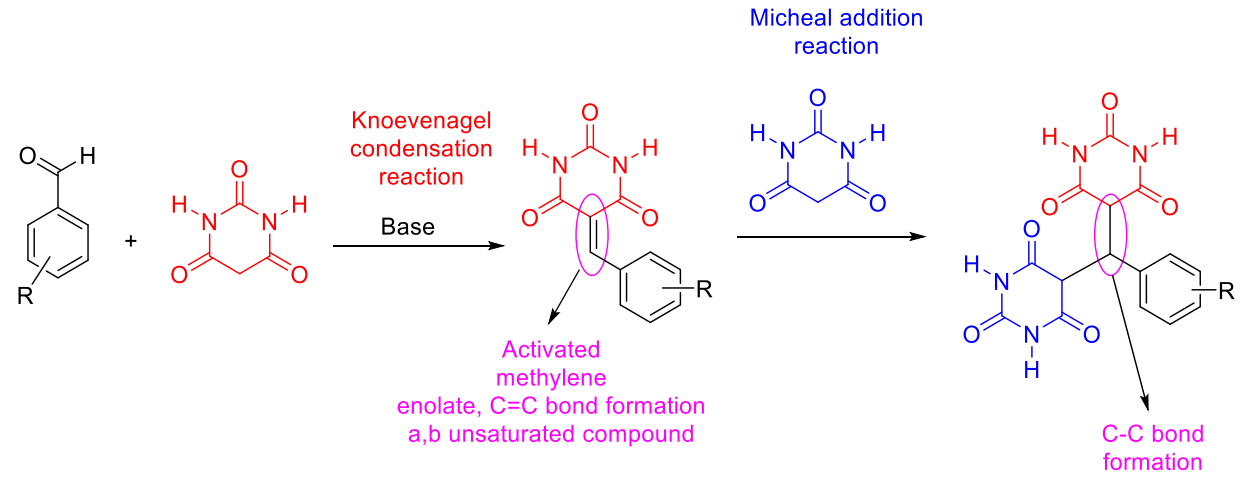

Figure 12**:** Knoevenagel condensation reaction followed by Michael addition reaction.[52]

5.4. Acylation reaction

Acylation reaction commonly refers to the introduction of an acyl group (R-C=O) to a molecule, where R is an alkyl group (aliphatic or alicyclic); the compound that provides the acyl group in acylation reaction is called “acylating agent”.[53]

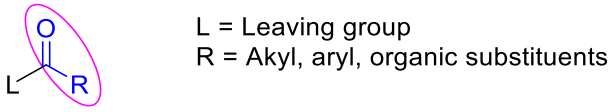

Figure 13: General structure Acyl group.

An acylation of BA at position C5 has been reported to have various biological potency. In this regard, Sakai *et al*. in 2002 reported library of acylation reactions using barbituric acid along with various acyl groups. The synthesis involved condensation reaction of barbituric acid derivatives represented by structure A below (Figure 14) and an acylation agent (B) such as acyl halides, acids anhydride, carboxylic acids, etc., in presence of a tertiary amine like triethylamine, diisopropylamine and *N*-methyl pyrrolidine.[54]

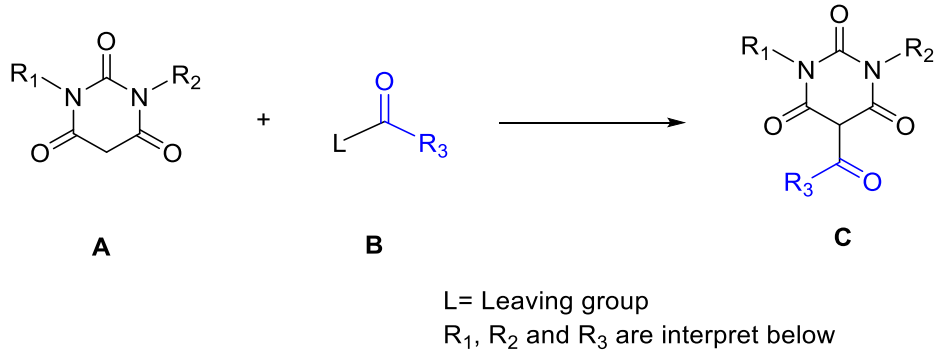

Figure 14: General Acylation reaction of barbituric acid derivatives

5.5. Thioamide synthesis reaction

Thioamides (general structure: R_1-CS-NR_2R_3 where R_1, R_2, and R_3 are an aliphatic or aromatic group as shown in Figure 15) are functional groups for the preparation of a number of biological relevant heterocycles scaffolds.[55] Some thioamides are known as plant protection agents or drugs,[56] others are used as ligands in coordination chemistry.[56] The first method for thioamide synthesis was introduced in 1878 by Hoffman which involved thionation of amides by phosphorus pentasulfide or Lawesson reagent. [57]

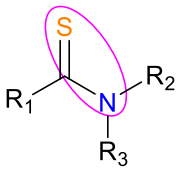

R_1, R_2 and R_3 are organic compounds

Figure 15: General structure of thioamide

However, in 1988, Jagodzinski *et al*. developed a direct synthesis of thioamides by reacting aromatic isothiocyanate with substituted benzenes and phenol in a nitromethane solution of aluminum chloride (Figure 16).[58]

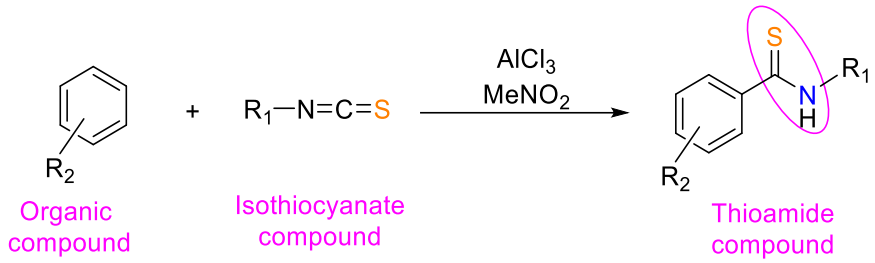

Figure 16: Thioamide compound formation.

The chemical and physical properties of thioamides are determined by the two active centers, one of them is associated with the nitrogen atom carrying a lone pair of the electron, and the other one is localized on the thiocarbonyl group.[56]

In the literature, Pancechowska-ksepko *et al*, 2008 reported some piperazine derivatives contains thioamides group that show some biological activity. These compound were studied against anaerobic bacteria of Gram-positive and Gram-negative, the minimal inhibitory concentration for these compounds **A**, **B**, **C,** and **D** were compared with the MIC of standard Metronidazole at low concentrations 6.2-12.5 µg/mL.[59] The derivatives studied showed distinguished activity towards the anaerobic bacteria but the maximum activity was exhibited by the compounds D.[59]

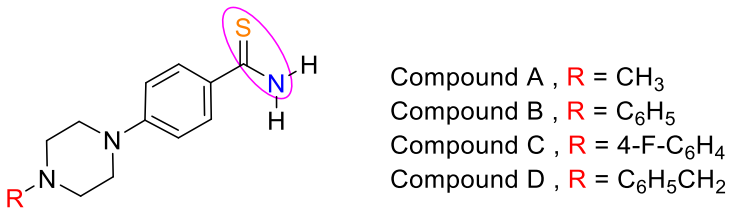

Figure 20: Piperazine derivatives with thioamides group.[59]

6. Spectroscopic characterization

Characterization of compounds to be used in a medicinal chemistry program should be conducted carefully to assure their structure. In this regard, TBA derivatives have been characterized using various spectroscopic techniques such as Nuclear Magnetic Resonance spectroscopy (NMR), Ultra-violet spectroscopy (UV), Infra-Red spectroscopy (IR), Single X-Ray Crystallography.

Nuclear magnetic resonance (NMR) is the most important analytical spectroscopic technique which helps chemists to elucidate the structure of synthesized compounds, for the advancement of organic chemistry.[60] It is based on the magnetic properties of the nuclei of atoms (such as Proton in case of ^{1}H NMR and Carbon for ^{13}C NMR).[61] The acetylated thiobarbituric acid analogs at C5 position are known to form the Keto-enol tautomerism, which can be elucidated well by temperature dependent NMR analysis in different solvents.[62] It has been shown by our research group earlier that enol form is more stable than keto derivative in case of acetylated barbituric acid.[62]

Another analytical tool, Ultraviolet spectroscopy which helps in determining the bonding patterns by using electron transition, is defined as the measurement of the attenuation of a beam of light after it passes through a sample or after reflection from the sample.[63] Most organic compounds have a different unsaturated functional group (alkene, aromatic compound, a compound with a carbonyl group, etc.) and UV-spectroscopy is used to detect the wavelength of these unsaturated functional group. The thiobarbituric derivatives are non-aromatic structurally but absorb UV on the TLC plate. This gives us the reason to study more and test their UV-absorption in different solvents (such as acetonitrile, ethanol, and dichloromethane).

Infra-Red (IR) spectroscopy helps in determining a functional group of compounds by stretching and bending vibrations of each bond in the molecule and report the absorption bands using wavenumbers.[63] It helps in the detection of specific functional groups as they are present as a characteristic band in the IR spectrum.

X-ray crystallography is a technique for determining the three-dimensional structure of the molecules in space.[64] This helps in better understanding of the derivatives structure along with the

presence of hydrogen bond donors and acceptors which can provide an insight into the explanation of biological activity.

Bearing all these in mind, here we explored TBA as a scaffold for the development of new antibacterial agents followed by their complete characterization using the above-explained spectroscopic techniques.

7. References

1. Butler, M. S.; Blaskovich, M. A.; Cooper, M. A., Antibiotics in the clinical pipeline at the end of 2015. *The Journal of antibiotics* **2017,** *70* (1).
2. Savoia, D., New antimicrobial approaches: reuse of old drugs. *Current drug targets* **2016,** *17* (6).
3. Cohen, M. L., Epidemiology of drug resistance: implications for a post-antimicrobial era. *Science* **1992,** *257* (5073).
4. El-Bashiti, T.; Jouda, M. M.; Masad, A., The Antimicrobial Effect of Some Medicinal Plant, and Interactions with Non-Antibiotics. *World Journal of Pharmacy and Pharmaceutical Sciences* **2016,** *5* (12).
5. López-Muñoz, F.; Ucha-Udabe, R.; Alamo, C., The history of barbiturates a century after their clinical introduction. *Neuropsychiatric Disease and Treatment* **2005,** *1* (4).
6. Scheele, K. W., Examen chemicum calculi urinarii. *Opuscula* **1776,** *2* (73).
7. Wöhler, F.; Liebig, J., Untersuchungen über die Natur der Harnsäure. *Annalen der Pharmacie* **1838,** *26* (3).
8. Schlieper, A., Ueber Alloxan, Alloxansäure und einige Neue Zersetzungsproducte der Harnsäure. *Justus Liebigs Annalen der Chemie* **1845,** *55* (3).
9. Carter, M. K., The story of barbituric acid. *Journal of Chemical Education* **1951,** *28* (10).
10. Baeyer, A., Untersuchungen über die Harnsäuregruppe. *Justus Liebigs Annalen der Chemie* **1863,** *127* (2).
11. Grimaux, E., Synthese des dérivés unique de la série de alloxan. Journal de *Bulletin de la Societe Chimique France* **1879.**
12. Mihic, S. J.; Harris, R. A., Hypnotics and sedatives. *Goodman & Gilman's The Pharmacological Basis of Therapeutics. 12th ed. New York, USA: McGraw-Hill* **2011**.
13. Vieira, A. A.; Gomes, N. M.; Matheus, M. E.; Fernandes, P. D.; Figueroa-Villar, J. D., Synthesis and in vivo evaluation of 5-chloro-5-benzobarbiturates as new central nervous system depressants. *Journal of the Brazilian Chemical Society* **2011,** *22* (2).

14. Figueiredo, J.; Serrano, J. L.; Cavalheiro, E.; Keurulainen, L.; Yli-Kauhaluoma, J.; Moreira, V. M.; Ferreira, S.; Domingues, F. C.; Silvestre, S.; Almeida, P., Trisubstituted barbiturates and thiobarbiturates: Synthesis and biological evaluation as xanthine oxidase inhibitors, antioxidants, antibacterial and anti-proliferative agents. *European Journal of Medicinal Chemistry* **2018,** *143*.
15. Tabern, D.; Volwiler, E., Sulfur-containing barbiturate hypnotics. *Journal of the American Chemical Society* **1935,** *57* (10).
16. Novak, I.; Kovač, B., Electronic structure and biological activity: Barbiturates vs. thiobarbiturates. *Chemical physics letters* **2010,** *493* (4-6).
17. Furukawa, Y. In *European Patent Appl. EP 88, 413 (1983)*, Chem. Abstr, 1983; p 22688.
18. Cordato, D. J.; Herkes, G. K.; Mather, L. E.; Morgan, M. K., Barbiturates for acute neurological and neurosurgical emergencies–do they still have a role? *Journal of clinical neuroscience* **2003,** *10* (3).
19. Kliethermes, C. L.; Metten, P.; Belknap, J. K.; Buck, K. J.; Crabbe, J. C., Selection for pentobarbital withdrawal severity: correlated differences in withdrawal from other sedative drugs. *Brain research* **2004,** *1009* (1-2).
20. Basavaraja, H.; Jayadevaiah, K.; Hussain, M.; Kumar, V.; Basavaraj, P., Synthesis of novel piperazine and morpholine linked substituted pyrimidine derivatives as antimicrobial agents. *Journal of Pharmaceutical Sciences and Research* **2010,** *2* (1).
21. Faidallah, H. M.; Khan, K. A., Synthesis and biological evaluation of new barbituric and thiobarbituric acid fluoro analogs of benzenesulfonamides as antidiabetic and antibacterial agents. *Journal of Fluorine Chemistry* **2012,** *142*.
22. Rajashakar, V.; Saisree, K.; Sikender, M.; Naveen, S.; Madhava Reddy, B., ISSN 0975-413X CODEN (USA): PCHHAX.
23. Althaus, I. W.; Chou, K.-C.; Lemay, R. J.; Franks, K. M.; Deibel, M. R.; Kezdy, F. J.; Resnick, L.; Busso, M. E.; So, A. G.; Downey, K. M., The benzylthio-pyrimidine U-31,355, a potent inhibitor of HIV-1 reverse transcriptase. *Biochemical Pharmacology* **1996,** *51* (6).
24. Afzal, O.; Kumar, S.; Haider, M. R.; Ali, M. R.; Kumar, R.; Jaggi, M.; Bawa, S., A review on anticancer potential of bioactive heterocycle quinoline. *European journal of medicinal chemistry* **2015,** *97*.
25. Alam, O.; Khan, S. A.; Siddiqui, N.; Ahsan, W.; Verma, S. P.; Gilani, S. J., Antihypertensive activity of newer 1, 4-dihydro-5-pyrimidine carboxamides: Synthesis and pharmacological evaluation. *European journal of medicinal chemistry* **2010,** *45* (11).
26. Haldar, M. K.; Scott, M. D.; Sule, N.; Srivastava, D.; Mallik, S., Synthesis of barbiturate-based methionine aminopeptidase-1 inhibitors. *Bioorganic & medicinal chemistry letters* **2008,** *18* (7).

27. Venugopala, K. N.; Krishnappa, M.; Nayak, S. K.; Subrahmanya, B. K.; Vaderapura, J. P.; Chalannavar, R. K.; Gleiser, R. M.; Odhav, B., Synthesis and antimosquito properties of 2, 6-substituted benzo [d] thiazole and 2, 4-substituted benzo [d] thiazole analogues against Anopheles arabiensis. *European journal of medicinal chemistry* **2013,** *65*.
28. Yan, Q.; Cao, R.; Yi, W.; Chen, Z.; Wen, H.; Ma, L.; Song, H., Inhibitory effects of 5-benzylidene barbiturate derivatives on mushroom tyrosinase and their antibacterial activities. *European journal of medicinal chemistry* **2009,** *44* (10).
29. Jursic, B. S., A simple method for Knoevenagel condensation of α, β-conjugated and aromatic aldehydes with barbituric acid. *Journal of Heterocyclic Chemistry* **2001,** *38* (3).
30. Fernández, J. G.; Mellet, C. O., Chemistry and developments of N-thiocarbonyl carbohydrate derivatives: sugar isothiocyanates, thioamides, thioureas, thiocarbamates, and their conjugates. *Advances in Carbohydrate Chemistry and Biochemistry* **2000,** *55*.
31. VULPEŞ, D.; Putz, M. V.; Chiriac, A., QSAR STUDY ON THE ANAESTHETIC ACTIVITY OF SOME BARBITURATES AND THIOBARBITURATES. *Revue Roumaine de Chimie* **2009,** *54* (9).
32. Dhorajiya, B.; Bhuva, R.; Dholakiya, B., Design, Synthesis and Comparative Study of Anti-Microbial Activities on Barbituric Acid and Thiobarbituric Acid based Chalcone Derivatives Bearing the Pyrimidine Nucleus. *Chem Sci J* **2016,** *7*.
33. Dickey, J.; Gray, A., Barbituric acid. *Organic Syntheses* **1934**, 8-8.
34. Albericio, F.; Sharma, A.; Noki, S.; Zamisa, S. J.; Hazzah, H.; Almarhoon, Z. M.; El-Faham, A.; de la Torre, B. G., Exploiting Thiobarbituric Acid Scaffold for Antibacterial Activity. *ChemMedChem* **2018**.
35. Schiff, H., Condensation products of aldehydes and ketones with primary amines. *Ann. Suppl* **1864,** *343* (3).
36. Pfeiffer, P.; Buchholz, E.; Bauer, O., Innere Komplexsalze von Oxyaldiminen und Oxyketiminen. *Journal für Praktische Chemie* **1931,** *129* (1).
37. Al Zoubi, W., Solvent extraction of metal ions by use of Schiff bases. *Journal of Coordination Chemistry* **2013,** *66* (13).
38. Wood, S. M., Organic Chemistry, Second Edition (Loudon, Marc G.). *Journal of Chemical Education* **1989,** *66* (3).
39. Przybylski, P.; Huczynski, A.; Pyta, K.; Brzezinski, B.; Bartl, F., Biological properties of Schiff bases and azo derivatives of phenols. *Current Organic Chemistry* **2009,** *13* (2).
40. Bringmann, G.; Dreyer, M.; Faber, J., Dalsgaard, D Pw, Staerk, JW Jaroszewski, et al. Ancistrotanzanine C and related 5, 1/Jaroszewski JW, et al. Ancistrotanzanine C and related 5,

1/and 7, 3/coupled naphthylisoquinoline alkaloids from Ancistrocladus tanzaniensis. *J Nat prod* **2004,** *67* (5).

41. Imran, M.; Iqbal, J.; Iqbal, S.; Ijaz, N., In vitro antibacterial studies of ciprofloxacin-imines and their complexes with Cu (II), Ni (II), Co (II), and Zn (II). *Turkish journal of biology* **2007,** *31* (2).
42. Kalaivani, S.; Priya, N. P.; Arunachalam, S., Schiff bases: facile synthesis, spectral characterization, and biocidal studies. *IJABPT* **2012,** *3*.
43. Jerry, M., Advanced Organic Chemistry: Reactions Mechanisms and Structure. McGraw Hill Book Company: 1968.
44. Knoevenagel, E., Condensation von Malonsäure mit aromatischen Aldehyden durch Ammoniak und Amine. *Berichte der Deutschen chemischen Gesellschaft* **1898,** *31* (3).
45. Jones, G., The K noevenagel Condensation. *Organic reactions* **2004,** *15*.
46. Tsogoeva, S. B., Recent advances in asymmetric organocatalytic 1, 4-conjugate additions. *European journal of organic chemistry* **2007,** *2007* (11).
47. Little, R. D.; Masjedizadeh, M. R.; Wallquist, O.; Mcloughlin, J. I., The Intramolecular Michael Reaction. *Organic Reactions* **2004,** *47*.
48. Mather, B. D.; Viswanathan, K.; Miller, K. M.; Long, T. E., Michael addition reactions in macromolecular design for emerging technologies. *Progress in Polymer Science* **2006,** *31* (5).
49. Coe, B.; Grassam, H.; Jeffery, J.; Coles, S.; Hursthouse, M., Reactions of 1, 3-diethyl-2-thiobarbituric acid with aldehydes: formation of arylbis (1, 3-diethyl-2-thiobarbituric-5-yl) methanes† and crystallographic evidence for ground state polarisation in 1, 3-diethyl-5-[4-(dimethylamino) benzylidene]-2-thiobarbituric acid. *Journal of the Chemical Society, Perkin Transactions 1* **1999,** (17).
50. Tietze, L. F.; Beifuss, U., The knoevenagel reaction. *Comprehensive Organic Synthesis; Trost, BM, Fleming, I., Eds* **1991**.
51. Kunz, F.; Margaretha, P.; Polansky, O., STABILE ORGANISCHE ELEKTRISCH-NEUTRALE LEWIS-SAEUREN. *Chemischer Informationsdienst. Organische Chemie* **1970,** *1* (31).
52. Jursic, B. S.; Neumann, D. M., Preparation of 5, 5′-pyrilidene and 5, 5′-quinolidene bis-barbituric acid derivatives. *Journal of heterocyclic chemistry* **2003,** *40* (3).
53. Sarvari, M. H.; Sharghi, H., Reactions on a solid surface. A simple, economical and efficient Friedel− Crafts acylation reaction over zinc oxide (ZnO) as a new catalyst. *The Journal of organic chemistry* **2004,** *69* (20).
54. Sakai, K.; Satoh, Y., Barbituric acid derivative and preventive and therapeutic agent for bone and cartilage containing the same. Google Patents: 2002.

55. Takahata, H.; Yamazaki, T., Synthesis of heterocycles using thioamide groups. *ChemInform* **1988,** *19* (5).
56. Jagodziński, T. S., Thioamides as useful synthons in the synthesis of heterocycles. *Chemical reviews* **2003,** *103* (1).
57. Cava, M. P.; Levinson, M. I., Thionation reactions of Lawesson's reagents. *Tetrahedron* **1985,** *41* (22).
58. Jagodziński, T., A simple method for the synthesis of thiobenzamides by Friedel-Crafts reaction. *Synthesis* **1988,** *1988* (09).
59. Pancechowska-Ksepko, D.; Spalińska, K.; Foks, H.; Kędzia, A.; Wierzbowska, M.; Kwapisz, E.; Janowiec, M.; Zwolska, Z.; Augustynowicz-Kopeć, E., Synthesis and Antibacterial Activity of New 1, 4-Disubstituted Piperazine Derivatives. *Phosphorus, Sulfur, and Silicon* **2008,** *183* (5).
60. Roberts, J. D., *Nuclear magnetic resonance: applications to organic chemistry*. McGraw-Hill Book Company, Inc: 1959.
61. Brown, T. L.; LeMay Jr, H. E.; Bursten, B. E.; Murphy, C. J., *Chemistry: The central science*. Southeast: 1978.
62. Sharma, A.; Jad, Y. E.; Ghabbour, H. A.; de la Torre, B. G.; Kruger, H. G.; Albericio, F.; El-Faham, A., Synthesis, crystal structure and DFT studies of 1, 3-Dimethyl-5-propionyl pyrimidine-2, 4, 6 (1H, 3H, 5H)-trione. *Crystals* **2017,** *7* (1), 31.
63. Bruice, P. Y., Organic Chemistry 4th Edition. Irene Lee Case Western Reserve University Cleveland, OH. 2004. Prentice Hall.
64. Picknett, T. M.; Brenner, S., X-Ray Crystallography. In *Encyclopedia of Genetics*, Brenner, S.; Miller, J. H., Eds. Academic Press: New York, 2001; p 2154.

CHAPTER 2

Exploiting the Thiobarbituric Acid Scaffold for Antibacterial Activity

Anamika Sharma, Sikabwe Noki, Sizwe J. Zamisa, Heba A. Hazzah, Zainab M. Almarhoon, Ayman El-Faham, Beatriz G. de la Torre, Fernando Albericio

Published article

DOI: 10.1002/cmdc.201800414.

ChemMedChem Peer-reviewed Journal.

ChemPubSoc Europe

DOI: 10.1002/cmdc.201800414

CHEMMEDCHEM Full Papers

Exploiting the Thiobarbituric Acid Scaffold for Antibacterial Activity

Anamika Sharma,[a] Sikabwe Noki,[a] Sizwe J. Zamisa,[b] Heba A. Hazzah,[a, c] Zainab M. Almarhoon,[d] Ayman El-Faham,*[d, e] Beatriz G. de la Torre,*[f] and Fernando Albericio*[b, d, g, h]

Thiobarbituric acid (TBA) has been considered a privileged structure for developing antimicrobial agents. Diversity was obtained at positions N and at C5 through acylation, Schiff base formation, Knoevenagel condensation, and thioamide and enamine formation. The present work describes the synthesis of small libraries based on the TBA moiety and above-mentioned reactions. Preliminary antimicrobial activity screening of the prepared compounds against selected bacteria (both Gram-positive and -negative) showed the best results for the Boc-Phe-TBA derivative. These results could be useful for designing and building libraries based on other amino acids with distinct protecting groups.

Introduction

The development of new antimicrobial agents remains a primary goal of medicinal chemists to address the problem of increasing bacterial resistance gained by microorganisms.[1–3] In this regard, emerging infectious diseases and the increasing number of multi-drug-resistant microbial pathogens pose a serious threat to human health and a challenge for public health systems. Action plans released by the World Health Organization (WHO) recognize that development of new antibiotics, particularly those with new modes of action, is a major requirement to avert antimicrobial drug resistance.[4]

One of our research programs in this field addresses this need with structures that are not known to be antibiotics (synthetic or natural medicinal compounds).[5,6] Although barbituric acid (BA) and, to a lesser extent, thiobarbituric acid (TBA) analogues have long been explored as privileged structures for a broad number of biological targets, they have found extensive application as antianxiety agents in the central nervous system.[7] In this regard, BA and TBA analogues exert their action by binding to receptors, which are ligand-gated ion channels.[8,9] It was previously reported that substitution at position 5 (C5) is critical in modulating the bioactivity of BA and TBA (Figure 1). Thus, substitution by alkyl or aryl groups at C5 enhances binding of the molecule to the γ-amino butyric acid (GABA) receptor. Furthermore, to conserve antianxiolytic activity, the compound must have at least one unsubstituted nitrogen atom.

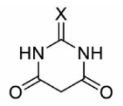

X = O: barbituric acid
X = S: thiobarbituric acid

Figure 1. General structure of BA and TBA.

In addition, BA and TBA exhibit a wide range of biological activities, including antiepileptic,[10] anticancer,[11–13] antioxidant,[14] anticonvulsant,[15] immunomodulatory,[12] gelatinase-inhibiting,[16] HIV integrase-inhibiting,[17] antifungal,[18] antiviral,[19] tyrosinase-inhibiting,[20,21] anti-inflammatory,[22] and antidiabetic[23] effects. BA and TBA derivatives have also been evaluated for antimicrobial activity.[23–26] 5-Benzylidene BA and TBA show antibacterial activity, as well as an inhibitory effect against mushroom tyrosinase.[27] However, TBA derivatives have been reported to show greater antibacterial activity than those derived from BA.[27–29] Substitution at C5 increases lipophilicity and hence facilitates the transport of BA and TBA analogues to their enzyme targets.[30,31]

[a] Dr. A. Sharma, S. Noki, Dr. H. A. Hazzah
School of Health Sciences, University of KwaZulu-Natal, University Road, Westville, Durban 4000 (South Africa)

[b] S. J. Zamisa, Prof. F. Albericio
School of Chemistry and Physics, University of KwaZulu-Natal, Private Bag X54001, Westville Campus, Durban 4000 (South Africa)
E-mail: albericio@ukzn.ac.za

[c] Dr. H. A. Hazzah
Department of Pharmaceutics, Faculty of Pharmacy and Drug Manufacturing, Pharos University in Alexandria, Alexandria 21641 (Egypt)

[d] Dr. Z. M. Almarhoon, Prof. A. El-Faham, Prof. F. Albericio
Department of Chemistry, College of Science, King Saud University, P.O. Box 2455, Riyadh 11451 (Saudi Arabia)
E-mail: aymanel_faham@hotmail.com

[e] Prof. A. El-Faham
Department of Chemistry, Faculty of Science, Alexandria University, P.O. Box 426, Alexandria 21321 (Egypt)

[f] Prof. B. G. de la Torre
KRISP, College of Health Sciences, University of KwaZulu-Natal, Westville, Durban 4001 (South Africa)
E-mail: garciadelatorreb@ukzn.ac.za

[g] Prof. F. Albericio
Department of Organic Chemistry, University of Barcelona, Martí i Franquès 1–11, 08028 Barcelona (Spain)

[h] Prof. F. Albericio
CIBER-BBN, Networking Centre on Bioengineering, Biomaterials and Nanomedicine, Barcelona Science Park, Baldiri Reixac 10, 08028 Barcelona (Spain)

Supporting information and the ORCID identification number(s) for the author(s) of this article can be found under: https://doi.org/10.1002/cmdc.201800414.

Bearing our own and others' results in mind, here we explored TBA as a scaffold for the development of new antibacterial agents. TBA has two potential reactive sites for exploring its structure activity relationship. One of our premises was to have substitution at the N position in order to avoid possible antianxiolytic properties. TBA analogues with N-substitution can be prepared using symmetrical substituted thiourea.[23,32,33] In contrast, protons at position C5 are highly acidic and hence undergo various reactions, including acylation and Knoevenagel condensation.[23] Furthermore, this highly acidic proton at the C5 position has also been explored to develop new derivatives of amino acid–TBA conjugates.

Results and Discussion

Chemistry

In the present study, we describe the synthesis of several derivatives based on the diethyl thiobarbituric acid (DETBA) moiety using different techniques as indicated below.

Acylation: Although BA acetylation can be achieved by several methods,[34] there is no appropriate or concrete evidence of TBA acetylation. Using DETBA as the substrate, acylation of TBA with acetic/propionic anhydride was performed following our previously reported method for BA with slight modifications[35,36] (Scheme 1). The use of aqueous media for this reaction and a small excess of anhydride is an advantage over the previously reported method.[34] Moreover, the method used herein can be considered a green method. The compounds (**A01** and **A02**) were obtained in high yields and were characterized by spectroscopic techniques. Prompted by these results, we also synthesized the benzoyl derivative by reacting benzoic anhydride with DETBA in a similar fashion as described above to afford **A03**; however, in this case, the yield obtained was lower than in preceding cases. This might be due to the lower activity of benzoic anhydride compared to acetic anhydride. **A01** and **A02** crystallized in their enol forms (crystallization of **A03** was not attempted), as shown by ^{1}H NMR (experimental section) and as reported earlier by our group for barbituric derivatives.[35]

To increase diversity, we acylated DETBA with N-protected amino acids. In this regard, we attempted to synthesize anhydrides of *tert*-butoxycarbonyl (Boc) amino acid and then reacted these with DETBA using a similar approach. However, the reactions gave almost negligible yields. After several attempts to prepare the convenient Boc amino acid derivative for acylation, **A04** and **A06** were obtained by in situ activation of Boc-AA-OH using 1-ethyl-3-(3-dimethylaminopropyl)carbodiimide (EDC), in the presence of *N*,*N*-dimethylaminopyridine (DMAP) and 1-hydroxybenzotriazole (HOBt), to afford the corresponding OBt ester, which reacted in situ with DETBA to give the corresponding products (Scheme 2). After Boc removal, these products afforded satisfactory yields of **A05** and **A07**.

Schiff bases: A reported method was used to prepare Schiff bases from **A01** with 2-picolylamine and 4-methoxybenzylamine. Satisfactory yields of compounds **A08** and **A09** were obtained, respectively (Scheme 3). The spectral data confirmed their enamine structures rather than imine structures, which were in good agreement with the reported data.[35,36]

Knoevenagel condensation: DETBA and related BA/TBA analogues undergo this reaction with aldehydes to yield 5-substituted products.[23,32] Interestingly, only the reaction of DETBA with 4-fluorobenzaldehyde cleanly gave the Knoevenagel condensation product. In contrast, for 3,5-dimethoxybenzaldehyde

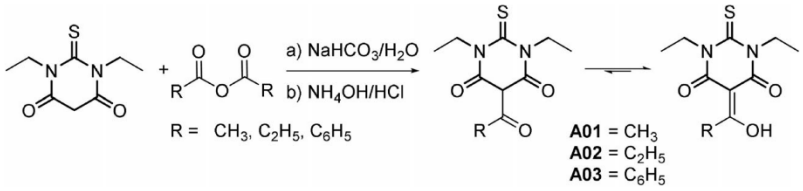

Scheme 1. Acetylation of thiobarbituric analogues.

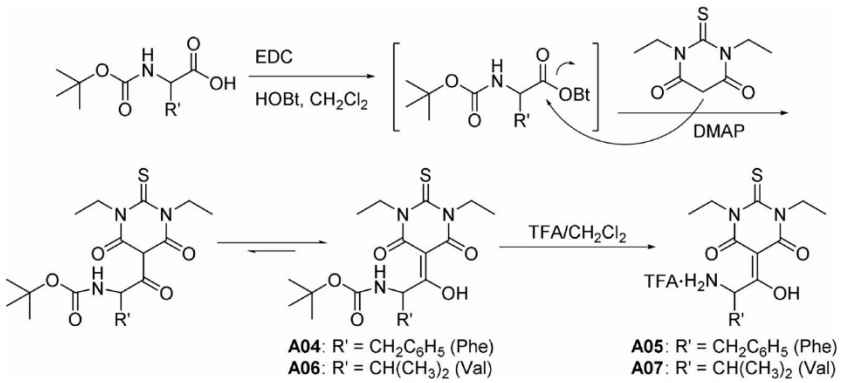

Scheme 2. Reaction of DETBA with Boc-AA-OH.

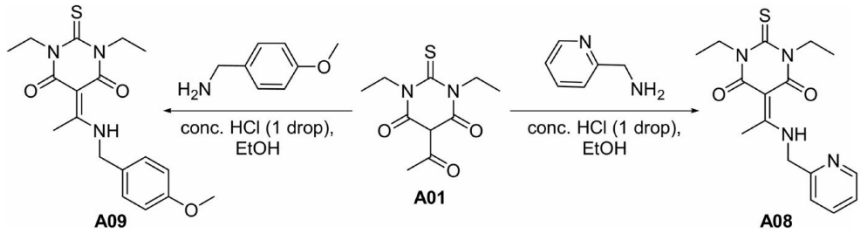

Scheme 3. Reaction of **A01** with amines (Schiff base synthesis).

and 2,4-dinitrobenzaldehyde, the Knoevenagel condensation was followed by Michael addition of the same DETBA. The pronounced difference with distinct aryl aldehydes may be due to electronic factors. Various factors controlling the Lewis acidity of Knoevenagel products are affected by either an increase in the electron-withdrawing nature of the substituent or in the planarity of the molecule,[37] which allows the product to further undergo Michael addition with another molecule of DETBA. The fluorine in 4-fluorobenzaldehyde is electron-withdrawing; however, it stabilizes the Knoevenagel product by extended conjugation, and hence, formation of the Michael addition product was not observed. In the case of 2,4-dinitrobenzaldehyde, the nitro group is strongly electron-withdrawing, thereby enhancing the Lewis acidity of the Knoevenagel product and leading to formation of the Michael addition product of DETBA (**A10**). Although the methoxy group is moderately electron-donating, it did not stabilize the Knoevenagel product and thus led to the Michael addition product (**A11** and **A12**) (Scheme 4).

Reaction with isothiocyanate: DETBA was reacted with *p*-tolyl isothiocyanate in the presence of base to yield **A13,** as reported in the literature,[38] with slight modifications and in good yield (Scheme 5).

N-Substituted thiobarbituric derivatives: N-substituted TBA can be obtained via the synthesis of symmetrical thiourea by condensation of an isothiocyanate with the corresponding amine. The resulting thiourea was further reacted with malonic acid and acetyl chloride at reflux. Using *p*-tolylisothiocyanate with *p*-toluidine, 2-thioxo-1,3-di-*p*-tolyldihydropyrimidine-4,6(1*H*,5*H*)-dione (MBTBA; **A14**) was formed. Acetylation of **A14** using acetic anhydride and propionic anhydride, following the same procedure as that used for **A01** and **A02**, resulted in 5-substituted MBTBA analogues **A15** and **A16**, respectively (Scheme 6). All derivatives were purified by recrystallization using ethanol as solvent.

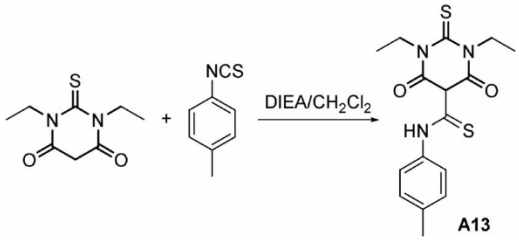

Scheme 5. Reaction of DETBA with *p*-tolylisothiocyanate.

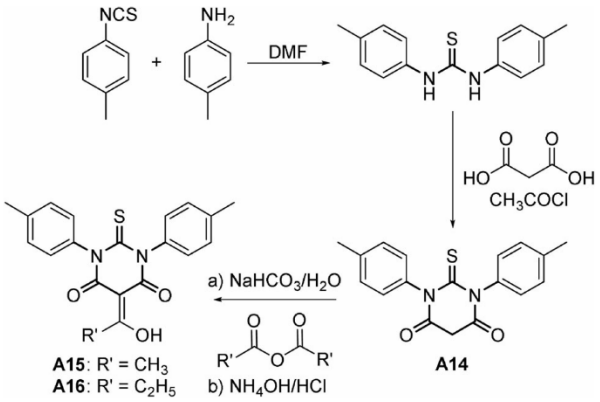

Scheme 6. Synthesis of MBTBA and further acylation using acetic anhydride/propionic anhydride.

Enamine formation: After recrystallization of the simple acyl derivatives (**A01**, **A02**, **A15**, **A16**) using ethanol as solvent, an extra derivative appeared by HPLC. This derivative increased in amount over time, and after several days, it was the only corresponding compound formed. It has been reported that ketones form imines in the presence of ammonium chloride and ethanol with a trace amount of water.[39] As expected, during

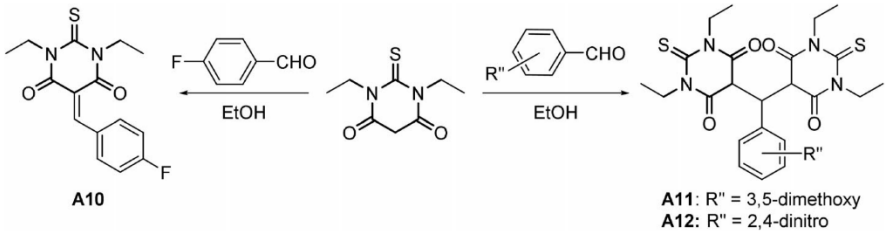

Scheme 4. Knoevenagel condensation in DETBA using substituted aryl benzaldehyde.

the workup, ammonium chloride formed as a result of the presence of NH_4OH and HCl (the first was added to solubilize the reaction mixture and the latter to precipitate the product). Thus, during the recrystallization step, full conversion of enol to enamine was achieved. The enamine (**A17**) was obtained in gram quantities and was confirmed by various spectroscopic techniques. In HPLC, the shift in retention time clearly indicated the formation of new derivative (i.e., the interconversion of enol to enamine). The conversion was confirmed by high-resolution mass spectrometry (HRMS) and NMR. This also provided concrete evidence that a trace amount of NH_4Cl (formed during workup) and ethanol as solvent during recrystallization are sufficient to achieve conversion of enol to enamine (Scheme 7). To avoid the formation of enamine and obtain only the enol, the recrystallization step was not performed, and the enol compounds (**A01**, **A02**, **A15**, **A16**) were isolated by freeze-drying to remove any traces of water.

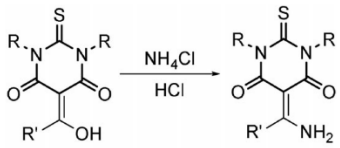

A01, A17: R = C_2H_5, R' = CH_3
A02, A18: R = C_2H_5, R' = C_2H_5
A15, A19: R = $C_6H_4CH_3$, R' = CH_3
A16, A20: R = $C_6H_4CH_3$, R' = C_2H_5

Scheme 7. Conversion of enol into enamine.

Antimicrobial activity

All derivatives obtained in this work were evaluated for antibacterial activity in terms of their minimum inhibitory concentration (MIC) against human pathogens *Staphylococcus aureus* (ATCC 29213) and *Bacillus subtilis* (ATCC 6051) as representatives of Gram-positive bacteria (Table 1), and *Escherichia coli* (ATCC 27853) and *Pseudomonas aeruginosa* (ATCC 27853) as Gram-negative bacteria. Meropenem was used as a positive control in the assays due to its broad range of activity against Gram-positive and -negative bacteria.

Table 1. MIC values for the synthesized derivatives against Gram-positive bacteria.

Compd	MIC [μg mL^{-1}]		Compd	MIC [μg mL^{-1}]	
	S. aureus ATCC 29213	*B. subtilis* ATCC 6051		*S. aureus* ATCC 29213	*B. subtilis* ATCC 6051
Std.[a]	0.25	0.25			
A01	32	32	**A11**	NI	NI
A02	32	32	**A12**	NI	NI
A03	NI	NI	**A13**	NI	NI
A04[b]	16	8	**A14**	NI	NI
A05	256	128	**A15**	NI	256
A06	32	32	**A16**	NI	NI
A07	NI	NI	**A17**	128	128
A08	NI	NI	**A18**	NI	NI
A09	NI	NI	**A19**	NI	NI
A10	NI	NI	**A20**	NI	NI

[a] Std.: meropenem. [b] **A04** was also tested against *S. epidermis* ATCC 14990 and *E. faecalis* ATCC 29212, giving MIC values of 4 and 8 μg mL^{-1}, respectively. NI: no inhibition.

No derivatives showed any antibacterial activity against the tested Gram-negative bacteria (*E. coli* and *P. aeruginosa*). As observed in Table 1, Compound **A01** and **A02** gave promising results against Gram-positive bacteria. On the other hand, the aromatic substitution resulted in a total loss of antimicrobial activity (**A03**). This observation confirmed that N-alkyl substitutions are preferred over aromatic substitutions, while acyl derivatives have more enhanced antibacterial activity than aromatic derivatives.

The two Boc-protected amino acids (**A04** and **A06**) exhibited antimicrobial activity, with **A04** having more activity than **A06**. This indicated that the type of amino acid has a great impact on the antimicrobial activity of DETBA derivatives. Accordingly, **A04** was further tested against *Staphylococcus epidermidis* (ATCC 14990) and *Enterococcus faecalis* (ATCC 29212), with MIC values of 4 and 8 μg mL^{-1}, respectively, that confirm its promising antibacterial properties. **A05** and **A07**, which were obtained by Boc group removal, showed near-total and total loss of activity, respectively. These observations could be attributed to the positive charge present on the amino group under physiological pH.

Further studies were performed on enamine products **A17**–**20**. We expected that the presence of the thiol group in the BA would increase the antimicrobial activity of the resulting products. Interestingly, enamine derivatives **A17**–**20** did not show any activity, and these results agreed with similar compounds derived from BA derivatives and reported by Neumann et al.[32] Furthermore, Schiff base derivatives (**A08** and **A09**), Knoevenagel condensation products (**A10**, **A11**, **A12**, and **A13**), and the aryl analogues of **A01** and **A02** (**A15** and **A16**) did not show any activity against Gram-positive or -negative bacteria.

The hemolytic activities of the three active derivatives (**A01**, **A04**, and **A06**) were tested as a gauge of cytotoxicity. DMSO was used as control, as the derivatives were soluble in DMSO. Figure 2 illustrates the hemolysis results. It can be clearly seen that at 1000 μg mL^{-1}, the hemolysis for **A01**, **A04**, and **A06** was 14.3, 8.3, and 8.5 %, respectively which dropped to 0, 0.6, and 2.3 %, respectively at 100 μg mL^{-1}. This indicated the nontoxicity of the tested derivatives.

All compounds showed poor solubility, which further prompted us to evaluate the antibacterial activity of two representative derivatives—**A01**, which showed activity, and **A17**, which was inactive—encapsulated in liquid crystalline nanoparticles of particle size 166 and 189 nm, respectively. The zeta potential was recorded as −20 and −12 mV respectively, thereby indicating the physical stability of the prepared dispersion. This was conducted to ensure that the loss in activity was not due to a solubility issue. However, the same results were obtained with liquid crystalline nanoparticles. These findings thus confirmed that the activity of the compounds did not depend on their solubility.

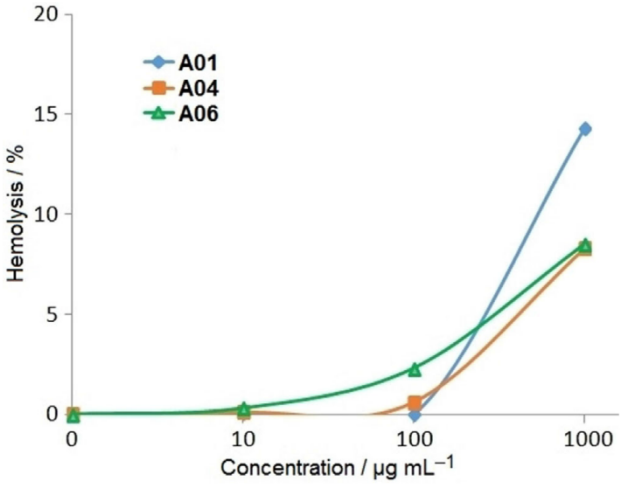

Figure 2. Hemolytic activity of **A01**, **A04**, and **A06**.

Conclusions

In conclusion, we demonstrated the potential of DETBA as a scaffold for the development of several derivatives obtained by different techniques, such as substitution at position N and at C5 through acylation, Schiff base formation, Knoevenagel condensation, thioamide formation, and enamine formation. Antibacterial activity, as evaluated against selected bacterial strains showed that N-alkyl derivatives and acyl derivatives of TBA exhibited greater activity than the aromatic derivatives. The type of amino acid also had a great effect on activity; that is, phenylalanine derivatives had greater activity than valine derivatives. Furthermore, the cytotoxic results from the active derivatives revealed they were nontoxic. These results present the possibility of building libraries based on other amino acids with distinct protecting groups that may be useful as new antibacterial agents.

Experimental Section

General

All reagents and solvents were purchased from commercial suppliers and were used without further purification, unless otherwise stated. PECEOL (glycerol mono-oleates, type 40) was a kind gift from Gattefosse, France. NMR spectra (^{1}H NMR and ^{13}C NMR) were recorded on a Bruker AVANCE III 400 MHz spectrometer. Chemical shift values are expressed in parts per million (ppm). Analytical HPLC was performed on an Agilent 1100 system using a Phenomenex C_{18} column (3 μm, 4.6×50 mm), and Chemstation software was used for data processing over a 5–95% gradient of CH_3CN (0.1% TFA)/H_2O (0.1% TFA) over 15 min, flow rate: 1.0 mL min^{-1}, detection at 220 nm. HRMS was performed using a Bruker ESI-QTOF mass spectrometer in positive ion mode.

Synthesis

Synthesis of diethyl TBA derivatives (A01 and A02): DETBA (10 mmol) was suspended in small amount of water, and a concentrated aqueous solution of sodium bicarbonate ($NaHCO_3$, 10 mmol) was added. After gas evolution ceased, acetic anhydride/propionic anhydride (5 equiv) was added to the stirred solution. A pale-yellow precipitate was formed after 10 min, and the mixture was stirred overnight. The residue was dissolved in ammonium hydroxide (NH_4OH). Hydrochloric acid (HCl) was added until the pH was below 1; the temperature of the solution rose, and the resulting precipitate was filtered and allowed to dry at room temperature to afford a pale-white solid.

5-Acetyl-1,3-diethyl-2-thioxodihydropyrimidine-4,6(1*H*,5*H*)-dione (A01): Pale-white solid (82% yield): mp: 40–42 °C; HPLC t_R= 11.9 min; ^{1}H NMR (400 MHz, [D$_6$]DMSO): δ=1.18 (t, J=7.0 Hz, -CH_3), 2.65 (s, -CH_3), 4.40 ppm (q, J=7.0 Hz, -CH_2); ^{13}C NMR (100 MHz, [D$_6$]DMSO): δ=11.8, 24.5, 42.5, 78.9, 97.4, 177.1, 197.3 ppm; HRMS *m/z*: calcd for $C_{10}H_{14}N_2O_3S$: 243.0798 $[M+H]^+$, found: 243.0811.

1,3-Diethyl-5-propionyl-2-thioxodihydropyrimidine-4,6(1*H*,5*H*)-dione (A02): Pale-white solid (56% yield): mp: 74–75 °C; HPLC t_R= 12.9 min; ^{1}H NMR (400 MHz, [D$_6$]DMSO): δ=1.14 (t, J=7.4 Hz, -CH_3), 1.19 (t, J=7.0 Hz, -CH_3), 3.11 (q, J=7.4 Hz, -CH_2), 4.41 ppm (q, J=7.0 Hz, -CH_2); ^{13}C NMR (100 MHz, [D$_6$]DMSO): δ=8.9, 11.8, 30.7, 42.6, 96.6, 171.6, 177.0, 201.4 ppm; HRMS *m/z*: calcd for $C_{11}H_{16}N_2O_3S$: 257.0954 $[M+H]^+$, found: 257.0966.

5-Benzoyl-1,3-diethyl-2-thioxodihydropyrimidine-4,6(1*H*,5*H*)-dione (A03): Benzoic acid was dissolved in dichloromethane (CH_2Cl_2), and *N*,*N*′-dicyclohexylcarbodiimide (DCC) was added in one portion, which resulted in the immediate formation of white precipitate. The reaction was stirred for 1 h at room temperature and then filtered using cotton to remove dicyclohexylurea (DCU). The filtrate was concentrated to afford benzoic anhydride. In parallel, DETBA (1 mmol) was suspended in small amount of water, and a concentrated aqueous solution of $NaHCO_3$ (1 mmol) was added. After gas evolution ceased, benzoic anhydride (5 equiv) was added to the stirred solution. A pale-yellow precipitate was formed after 10 min, and the mixture was stirred overnight. The precipitate was dissolved in NH_4OH. HCl was added until the pH was below 1; the temperature of the solution rose and the precipitate formed was filtered and allowed to dry at room temperature to yield a pale-white solid (36% yield): mp: 92–93 °C; HPLC t_R=13.1 min; ^{1}H NMR (400 MHz, [D$_6$]DMSO): δ=1.18 (t, J=7.0 Hz, -CH_3), 4.39 (q, J= 7.0 Hz, -CH_2), 7.4–7.6 ppm (m, Ar-H); ^{13}C NMR (100 MHz, [D$_6$]DMSO): δ=12.1, 42.3, 96.3, 127.6, 128.4, 131.4, 137.1, 161.6, 167.3, 177.0, 192.3 ppm; HRMS *m/z*: calcd for $C_{11}H_{16}N_2O_3S$: 305.0954 $[M+H]^+$, found: 305.0957.

Synthesis of A04 and A06: Boc-AA-OH (1 equiv) and EDC (1.3 equiv) were dissolved in CH_2Cl_2, and DETBA (1.5 equiv), triethyl amine (3 equiv), HOBt (0.6 equiv), and DMAP (0.5 equiv) were added. The reaction mixture was stirred at room temperature for 16 h. The solvent was concentrated, and the residue was dissolved in ethyl acetate. The organic layer was washed with sat. $NaHCO_3$, and brine (3×30 mL). It was then collected, concentrated, and poured into HCl (1 N). The resulting suspension was filtered, and the solid was washed with water and dried to afford pure compounds **A04** and **A06**.

***tert*-Butyl (1-(1,3-diethyl-4,6-dioxo-2-thioxohexahydropyrimidin-5-yl)-1-oxo-3-phenylpropan-2-yl)carbamate (A04)**: Pale-pink solid (94% yield): mp: 130–131 °C; HPLC t_R=14.4 min; ^{1}H NMR (400 MHz, [D$_6$]DMSO): δ=1.18 (t, J=7.2 Hz, -CH_3), 1.28 (s, -CH_3), 3.09–3.12 (m, -CH_2), 4.44 (q, J=7.2 Hz, -CH_2), 5.52 (t, J=7.8, -CH), 7.16 (d, J=7.3 Hz, -NH), 7.21–7.33 ppm (m, Ar-H); ^{13}C NMR (100 MHz, [D$_6$]DMSO): δ=12.4, 18.8, 28.1, 45.7, 60.2, 69.9, 71.9,

125.7, 127.7, 129.3, 138.9, 155.1, 177.1, 183.8, 216.1 ppm; HRMS m/z: calcd for $C_{11}H_{16}N_2O_3S$: 448.1900 $[M+H]^+$, found: 448.1901.

***tert*-Butyl (1-(1,3-diethyl-4,6-dioxo-2-thioxohexahydropyrimidin-5-yl)-3-methyl-1-oxobutan-2-yl)carbamate (A06)**: Dark-pink solid (92% yield): mp: 100–101 °C; HPLC t_R = 14.1 min; ^{1}H NMR (400 MHz, [D$_6$]DMSO): δ = 0.81 (d, J = 6.8 Hz, -CH$_3$), 1.18 (t, J = 6.6 Hz, -CH$_3$), 1.37 (s, -CH$_3$), 3.06–3.11 (m, -CH), 3.80 (s, -CH), 4.41 (q, J = 6.8 Hz, -CH$_2$), 5.52 (d, J = 7.3 Hz, -CH), 6.87 ppm (s, NH); ^{13}C NMR (100 MHz, [D$_6$]DMSO): δ = 11.9, 28.1, 30.1, 42.6, 52.1, 58.9, 78.1, 139.1, 155.6, 168.7, 176.8, 199.5 ppm; HRMS *m/z*: calcd for $C_{11}H_{16}N_2O_3S$: 400.1901 $[M+H]^+$, found: 400.1884.

Synthesis of A05 and A07: Compounds **A04** and **A06** were dissolved separately in trifluoroacetic acid (TFA), and the solution was stirred for 1 h at room temperature. The TFA was then removed to afford **A05** and **A07** as TFA salts.

1,3-Diethyl-5-phenylalanyl-2-thioxodihydropyrimidine-4,6(1*H*,5*H*)-dione (A05): Pale-pink sticky solid (98% yield): HPLC t_R = 7.6 min; ^{1}H NMR (400 MHz, [D$_6$]DMSO): δ = 1.15 (t, J = 6.8 Hz, -CH$_3$), 3.08–3.12 (m, -CH$_2$), 4.20 (t, J = 5.5 Hz, -CH), 4.40 (q, J = 6.8 Hz, -CH$_2$), 7.23–7.30 (m, Ar-H), 7.72 ppm (bs, -NH$_2$); ^{13}C NMR (100 MHz, [D$_6$]DMSO): δ = 12.5, 41.5, 53.1, 58.5, 95.0, 128.4, 128.6, 129.4, 136.5, 160.2, 176.7, 189.6 ppm; HRMS *m/z*: calcd for $C_{11}H_{16}N_2O_3S$: 348.1376 $[M+H]^+$, found: 348.1388.

1,3-Diethyl-2-thioxo-5-valyldihydropyrimidine-4,6(1*H*,5*H*)-dione (A07): Dark-pink sticky solid (97% yield): HPLC t_R = 6.6 min; ^{1}H NMR (400 MHz, [D$_6$]DMSO): δ = 0.76 (d, J = 7 Hz, -CH$_3$), 1.2 (t, J = 7 Hz, -CH$_3$), 2.16 (m, -CH), 3.10 (m, -CH), 4.37 (q, J = 7 Hz, -CH$_2$), 4.96 (d, J = 8.5 Hz, -CH), 7.66 ppm (bs, NH$_2$); ^{13}C NMR (100 MHz, [D$_6$]DMSO): δ = 12.5, 15.8, 19.6, 29.1, 41.5, 61.5, 160.1, 176.7, 190.5 ppm; HRMS *m/z*: calcd for $C_{11}H_{16}N_2O_3S$: 300.1376 $[M+H]^+$, found: 300.1377.

Synthesis of A08 and A09: Compound **A01** was dissolved in ethanol, and amine was added, followed by addition of one drop of conc. HCl. The reaction was stirred overnight at room temperature. After completion, the solvent was removed, and the residue was washed with diethyl ether, followed by purification using silica gel column chromatography to afford the pure product.

(*E*)-1,3-Diethyl-5-(1-((pyridin-2-ylmethyl)imino)ethyl)-2-thioxodihydropyrimidine-4,6(1*H*,5*H*)-dione (A08): Pale-yellow solid (sticky at room temperature; 86% yield): HPLC t_R = 8.8 min; ^{1}H NMR (400 MHz, CDCl$_3$): δ = 1.22 (t, J = 7.0 Hz, -CH$_3$), 2.69 (s, -CH$_3$), 4.49 (q, J = 7.0 Hz, -CH$_2$), 4.75 (d, J = 5.6 Hz, -CH$_2$), 7.2–8.6 (m, Ar-H), 13.3 ppm (s, -CH); ^{13}C NMR (100 MHz, CDCl$_3$): δ = 11.4, 17.9, 41.8, 42.2, 48.2, 92.3, 120.4, 122.1, 136.3, 148.9, 153.3, 174.3, 176.6 ppm; HRMS: *m/z*: calcd for $C_{11}H_{16}N_2O_3S$: 333.1380 $[M+H]^+$, found: 333.1387.

(*E*)-1,3-Diethyl-5-(1-((4-methoxybenzyl)imino)ethyl)-2-thioxodihydropyrimidine-4,6(1*H*,5*H*)-dione (A09): White solid (69% yield): mp: 98–100 °C; HPLC t_R = 12.6 min; ^{1}H NMR (400 MHz, CDCl$_3$): δ = 1.21 (t, J = 6.9 Hz, -CH$_3$), 2.10 (s, -OCH$_3$), 2.66 (s, -CH$_2$), 3.75 (s, -CH$_3$), 4.47 (q, J = 7.0 Hz, -CH$_2$), 6.84–7.15 (m, Ar-H), 12.96 ppm (s, -CH); ^{13}C NMR (100 MHz, CDCl$_3$): δ = 11.4, 17.2, 41.8, 42.6, 46.8, 54.9, 113.7, 127.4, 130.1, 152.1, 154.4, 167.4, 173.6 ppm; HRMS *m/z*: calcd for $C_{11}H_{16}N_2O_3S$: 362.1533 $[M+H]^+$, found: 362.1535.

Synthesis of A10, A11, A12: DETBA and aldehyde were dissolved in ethanol and stirred at room temperature for 10 min. A precipitate formed. The reaction was monitored for complete consumption of the starting material, and the solvent was then removed to afford the pure product.

1,3-Diethyl-5-(4-fluorobenzylidene)-2-thioxodihydropyrimidine-4,6(1*H*,5*H*)-dione (A10): Yellow solid (70% yield): mp: 180–182 °C; HPLC t_R = 11.9 min; ^{1}H NMR (400 MHz, CDCl$_3$): δ = 1.30 (t, J = 7.0 Hz, -CH$_3$), 4.59 (q, J = 7.0 Hz, -CH$_2$), 7.00–7.04 (m, Ar-H), 13.86 ppm (s, -CH); ^{13}C NMR (100 MHz, CDCl$_3$): δ = 12.1, 45.2, 97.4, 115.2, 115.4, 127.9, 128.0, 162.2, 163.7, 174.6 ppm; HRMS *m/z*: calcd for $C_{11}H_{16}N_2O_3S$: 307.0911 $[M+H]^+$, found: 307.0908.

5,5′-((3,5-Dimethoxyphenyl)methylene)bis(1,3-diethyl-2-thioxodihydropyrimidine-4,6(1*H*,5*H*)-dione) (A11): Yellow solid (74% yield): mp: 150–151 °C; HPLC t_R = 13.1 min; ^{1}H NMR (400 MHz, [D$_6$]DMSO): δ = 1.16 (t, J = 7.0 Hz, -CH$_3$), 3.44 (m, -CH), 3.62 (s, -OCH$_3$), 4.45 (q, J = 7.0 Hz, -CH$_2$), 6.10–6.26 (m, Ar-H), 8.10 ppm (d, J = 6.6, -CH); ^{13}C NMR (100 MHz, [D$_6$]DMSO): δ = 12.3, 18.5, 33.6, 42.8, 54.8, 96.3, 104.9, 145.2, 160.1, 161.1, 174.0 ppm; HRMS *m/z*: calcd for $C_{11}H_{16}N_2O_3S$: 549.1836 $[M+H]^+$, found: 549.1821.

5,5′-((2,4-Dinitrophenyl)methylene)bis(1,3-diethyl-2-thioxodihydropyrimidine-4,6(1*H*,5*H*)-dione) (A12): Off-white solid (76% yield): mp: 163–165 °C; HPLC t_R = 12.2 min; ^{1}H NMR (400 MHz, [D$_6$]DMSO): δ = 1.14 (t, J = 6.7 Hz, -CH$_3$), 4.40 (q, J = 6.7 Hz, -CH$_2$), 6.42 (s, -CH), 7.51–8.41 ppm (m, Ar-H); ^{13}C NMR (100 MHz, [D$_6$]DMSO): δ = 12.1, 32.3, 42.8, 94.2, 118.9, 125.6, 130.9, 143.4, 145.5, 149.3, 160.7, 174.4 ppm; HRMS *m/z*: calcd for $C_{11}H_{16}N_2O_3S$: 579.1326 $[M+H]^+$, found: 579.1322.

1,3-Diethyl-4,6-dioxo-2-thioxo-*N*-(*p*-tolyl)hexahydropyrimidine-5-carbothioamide (A13): DETBA and *p*-tolyl isothiocyanate were dissolved in CH_2Cl_2, and DIEA was added. The reaction was stirred overnight at room temperature. The reaction mixture was washed with HCl (1 N), and the organic layer was collected, dried over $MgSO_4$, filtered, and concentrated to afford the pure product as a pale-yellow solid (90% yield): mp: 132–133 °C; HPLC t_R = 15.6 min; ^{1}H NMR (400 MHz, [D$_6$]DMSO): δ = 1.31 (t, J = 7.0 Hz, -CH$_3$), 2.39 (s, -CH$_3$), 4.58 (q, J = 7.0, -CH$_2$), 7.31–7.39 (m, Ar-H), 13.9 ppm (s, -NH); ^{13}C NMR (100 MHz, [D$_6$]DMSO): δ = 11.6, 20.7, 43.8, 91.7, 125.2, 129.5, 134.5, 137.0, 174.3, 184.9, 202.9 ppm; HRMS *m/z*: calcd for $C_{11}H_{16}N_2O_3S$: 350.0991 $[M+H]^+$, found: 350.0962.

Synthesis of 2-thioxo-1,3-di-*p*-tolyldihydropyrimidine-4,6(1*H*,5*H*)-dione (A14): A mixture of *p*-toluidine (10 mmol) in DMF (20 mL) and *p*-tolyl isothiocyanate (10 mmol) in dioxane (20 mL) was heated for 1 h. The reaction mixture was then cooled and poured into ice cooled water to afford a pale-yellow solid. The solid was filtered, washed with water, and dried to afford pure 1,3-di-*p*-tolylthiourea, which was further used without purification. Methyl malonic acid was added to 1,3-di-*p*-tolylthiourea, and the mixture was dissolved in acetyl chloride. The reaction was heated at 40 °C for 12 h and was then cooled and poured onto crushed ice. The solid was filtered, washed with water, and dried to afford pure **A14** as a yellow solid (92% yield): mp: 218–220 °C; HPLC t_R = 10.2 min; ^{1}H NMR (400 MHz, [D$_6$]DMSO): δ = 2.27 (s, -CH$_3$), 7.12 (d, J = 8.1 Hz Ar-H), 7.33 (d, J = 8.1 Hz, Ar-H), 9.58 ppm (s, -CH$_2$); ^{13}C NMR (100 MHz, [D$_6$]DMSO): δ = 21.1, 40.6, 128.4, 129.5, 136.6, 137.9, 169.3, 174.2 ppm; HRMS *m/z*: calcd for $C_{11}H_{16}N_2O_3S$: 325.1005 $[M+H]^+$, found: 325.1025.

Synthesis of A15 and A16: A mixture of **A14** and acetic anhydride/propionic anhydride with a few drops of conc. sulfuric acid was stirred at reflux for 1 h. The reaction mixture was then concentrated to half its volume and cooled to 0 °C. The resulting solid was then filtered, washed with water, and dried to afford pure products **A15** and **A16**.

5-Acetyl-2-thioxo-1,3-di-*p*-tolyldihydropyrimidine-4,6(1*H*,5*H*)-dione (A15): Yellow solid (45% yield): mp: 185–186 °C; HPLC t_R =

12.0 min; ^{1}H NMR (400 MHz, [D$_6$]DMSO): δ = 2.34 (s, -CH$_3$), 2.65 (s, -CH$_3$), 7.15 (d, J = 8.2 Hz Ar-H), 7.26 ppm (d, J = 8.2 Hz, Ar-H); ^{13}C NMR (100 MHz, [D$_6$]DMSO): δ = 20.7, 24.5, 98.2, 128.5, 129.5, 136.7, 137.6, 179.6, 196.3, 206.9 ppm; HRMS m/z: calcd for $C_{11}H_{16}N_2O_3S$: 367.1077 $[M+H]^+$, found: 367.1100.

5-Propionyl-2-thioxo-1,3-di-*p*-tolyldihydropyrimidine-4,6(1*H*,5*H*)-dione (A16): Yellow solid (57% yield): mp: 140–141 °C; HPLC t_R = 12.7 min; ^{1}H NMR (400 MHz, [D$_6$]DMSO): δ = 1.14 (t, J = 7.4 Hz, -CH$_3$), 2.33 (s, -CH$_3$), 2.91 (q, J = 7.4 Hz, -CH$_2$), 7.08 (d, J = 8.2 Hz, Ar-H), 7.20 ppm (d, J = 8.2 Hz, Ar-H); ^{13}C NMR (100 MHz, [D$_6$]DMSO): δ = 10.1, 20.7, 30.1, 63.4, 128.5, 129.5, 137.6, 166.2, 170.6, 179.5, 187.6 ppm; HRMS: m/z: calcd for $C_{11}H_{16}N_2O_3S$: 381.1290 $[M+H]^+$, found: 381.1267.

Synthesis of enamines formed during recrystallization (A17, A18, A19, and A20)

5-(1-Aminoethylidene)-1,3-diethyl-2-thioxodihydropyrimidine-4,6(1*H*,5*H*)-dione (A17): Yellow solid; mp: 190–191 °C; HPLC t_R = 9.2 min; ^{1}H NMR (400 MHz, [D$_6$]DMSO): δ = 1.14 (t, J = 7 Hz, -CH$_3$), 2.53 (s, -CH$_3$), 4.37 (q, J = 7 Hz, -CH$_2$), 9.7 (s, -NH$_2$), 11.1 ppm (s, -NH$_2$); ^{13}C NMR (100 MHz, [D$_6$]DMSO): δ = 12.1, 24.3, 42.0, 91.2, 175.8, 176.9, 197.3 ppm; HRMS m/z: calcd for $C_{11}H_{16}N_2O_3S$: 242.0958 $[M+H]^+$, found: 242.0966.

5-(1-Aminopropylidene)-1,3-diethyl-2-thioxodihydropyrimidine-4,6(1*H*,5*H*)-dione (A18): Yellow solid; mp: 101–102 °C; HPLC t_R = 10.1 min; ^{1}H NMR (400 MHz, [D$_6$]DMSO): δ = 1.15 (t, J = 7.3 Hz, -CH$_3$), 1.16 (t, J = 6.9 Hz, -CH$_3$), 2.53 (q, J = 7.3 Hz, -CH$_3$), 4.40 (q, J = 6.9 Hz, -CH$_2$), 9.68 (s, -NH$_2$), 11.18 ppm (s, -NH$_2$); ^{13}C NMR (100 MHz, [D$_6$]DMSO): δ = 12.2, 12.7, 29.2, 42.1, 90.3, 161.2, 176.9, 180.6 ppm; HRMS m/z: calcd for $C_{11}H_{16}N_2O_3S$: 256.1080 $[M+H]^+$, found: 256.1096.

5-(1-Aminoethylidene)-2-thioxo-1,3-di-*p*-tolyldihydropyrimidine-4,6(1*H*,5*H*)-dione (A19): Yellow solid; mp: 198–200 °C; HPLC t_R = 9.9 min; ^{1}H NMR (400 MHz, [D$_6$]DMSO): δ = 1.23 (s, -CH$_3$), 2.33 (s, -CH$_3$), 7.07 (d, J = 8.2 Hz, Ar-H), 7.20 (d, J = 8.2 Hz, Ar-H), 9.69 (s, -NH$_2$), 10.9 ppm (s, -NH$_2$); ^{13}C NMR (100 MHz, [D$_6$]DMSO): δ = 20.8, 23.4, 101.2, 129.8, 132.4, 136.2, 137.3, 162.8, 167.3, 172.5 ppm; HRMS m/z: calcd for $C_{11}H_{16}N_2O_3S$: 366.1282 $[M+H]^+$, found: 366.1271.

5-(1-Aminopropylidene)-2-thioxo-1,3-di-*p*-tolyldihydropyrimidine-4,6(1*H*,5*H*)-dione (A20): Yellow solid; mp: 159–160 °C; HPLC t_R = 10.6 min; ^{1}H NMR (400 MHz, [D$_6$]DMSO): δ = 1.14 (t, J = 7.4 Hz, CH$_3$), 2.33 (s, -CH$_3$), 2.91 (q, J = 7.4 Hz, CH$_2$), 7.08 (d, J = 8.2 Hz, Ar-H), 7.20 (d, J = 8.2 Hz, Ar-H), 9.62 (s, -NH$_2$), 10.97 ppm (s, -NH$_2$); ^{13}C NMR (100 MHz, [D$_6$]DMSO): δ = 9.8, 20.7, 24.5, 98.2, 128.5, 129.5, 136.7, 137.6, 162.4, 179.6, 196.3 ppm; HRMS m/z: calcd for $C_{11}H_{16}N_2O_3S$: 380.1436 $[M+H]^+$, found: 380.1427.

Biological activity

Compounds and reference bacterial strains: The compounds were dissolved in DMSO. ATCC bacterial strains (two Gram-positive and two Gram-negative) were subcultured on Mueller–Hinton agar and incubated at 37 °C for 24 h prior to use in the experiments.

Minimum inhibitory concentration (MIC) determination: MIC values were determined using the broth microdilution method, as described by the Clinical and Laboratory Standards Institute (CLSI) guidelines.[40] Briefly, twofold serial dilutions of each compound (4–256 μM) were created in cation-adjusted Mueller–Hinton broth (CAMHB) in a 96-well microtiter plate. The bacterial inoculum was prepared in distilled water and matched to a 0.5 McFarland standard and added to make a final volume of 200 μL in each microtiter well. The plates were incubated with shaking for 24 h at 37 °C under aerobic conditions. Alamar blue dye[41] was added to the wells and incubated for 1.5 h, with the color change indicating bacterial growth. The MIC was then recorded as the lowest concentration at which there was no visible growth. A drug-free well and media control well containing bacteria and CAMHB, respectively, were included in each plate. Meropenem was also tested as a drug control. The assay was performed in duplicate to confirm results.

Hemolytic activity: Fresh blood (10 mL) was collected in EDTA tubes and centrifuged at 1000 *g* for 10 min at 4 °C. After plasma removal, the pellet containing red blood cells (RBCs) was washed three times with phosphate-buffered saline (PBS; 35 mM phosphate, 150 mM NaCl, pH 7.4) and resuspended in PBS at a concentration of 8% (*v/v*). Derivatives **A01**, **A04**, and **A06** (100 μL each of 2000, 200, 20, and 2 μg mL^{-1}) were placed in a 96-well plate, followed by addition of RBC solution (100 μL), to give final concentrations of 4% (*v/v*) RBCs and 1000, 100, 10, and 1 μg mL^{-1} of the derivatives, respectively. After incubation at 37 °C for 30 min, samples were centrifuged at 1000 *g* for 2 min, supernatants were transferred to 96-well plates, and released hemoglobin was measured spectrophotometrically at 450 and 415 nm in an iMark microplate reader (California, USA). A 1% solution of Triton X-100 (untreated) was used as a positive control, and 4% RBCs was used as a negative control. Also, DMSO was tested at the same percentage as used to solubilize the compounds. The percentage of hemolysis was determined as $[OD_{nm}(\text{treated})-OD_{nm}(\text{untreated})]/[OD_{nm}(\text{Triton})-OD_{nm}(\text{untreated})]\times 100$. Experiments were carried out in triplicate.

Preparation of liquid crystalline nanoparticles (LCNPs) by emulsification: Preparation of **A01**- and **A17**-loaded LCNPs was based on the emulsification of mixtures of glyceryl monoolein and the surfactant in water as described in the literature.[42] An appropriate amount of glyceryl monoolein (MO) (6%, *w/v*) and poloxamer-407 (P-407) (1%, *w/v*) with respect to the aqueous dispersion were melted in a water bath at 65 °C. The molten mixture containing the calculated amount of **A01** and **A17** (0.15%) was then added dropwise in parallel to a preheated aqueous phase at 65 °C and stirred on a magnetic stirrer for 15 min. The dispersion was then sonicated for 10 min using a probe sonicator at a maximum power of 40 V until a uniform opaque white mixture without aggregates was formed. A placebo formula free of drug was also prepared following the same procedure.

Characterization of drug-loaded LCNPs: Dynamic light scattering technique using a Malvern zetasizer was used to determine the particle size and polydispersity index (PDI) of the prepared formulations. Before the analysis, each sample was diluted with deionized water (1:100). All measurements were performed in triplicate.

Zeta potential (ZP) measurements: ZP values were calculated using a Malvern zetasizer. Before each determination, samples were diluted with deionized water (1:100). All determinations were performed in triplicate.

Acknowledgements

This work was funded by the South Africa National Research Foundation (NRF) Blue Sky's Research Programme (#110960), the University of KwaZulu-Natal, the International Scientific Partner-

ship Program (ISPP) at King Saud University (#0061), the Spanish Ministry of Economy, Industry and Competitiveness (MINECO; CTQ2015-67870-P), and the Generalitat de Catalunya (2014 SGR 137).

Conflict of Interest

The authors declare no conflict of interest.

Keywords: antibiotics · barbituric acid · nanoformulations · thiobarbituric acid

[1] T. El-Bashiti, M. M. Jouda, A. Masad, *World J. Pharm. Pharm. Sci.* **2016**, *5*, 159 – 168.
[2] D. Savoia, *Curr. Drug Targets* **2016**, *17*, 731 – 738.
[3] M. O. Sommer, C. Munck, R. V. Toft-Kehler, D. I. Andersson, *Nat. Rev. Microbiol.* **2017**, *15*, 689 – 696.
[4] M. S. Butler, M. A. Blaskovich, M. A. Cooper, *J. Antibiot.* **2017**, *70*, 3 – 24.
[5] S. Kalayci, *EC Microbiol.* **2017**, *10*, 19 – 21.
[6] S. Kalayci, S. Demirci, F. Sahin, *Curr. Psychopharmacol.* **2014**, *3*, 195 – 202.
[7] G. Kapoor, D. Pathak, P. Bhutani, R. Kant, *J. Chem. Pharm. Res.* **2016**, *8*, 151 – 168.
[8] T. Morimoto, K. Sakamoto, H. Sade, S. Ohya, K. Muraki, Y. Imaizumi, *Mol. Pharmacol.* **2007**, *71*, 1075 – 1088.
[9] H. R. Arias, E. A. McCardy, M. J. Gallagher, M. P. Blanton, *Mol. Pharmacol.* **2001**, *60*, 497 – 506.
[10] A. Agarwal, S. Lata, K. Saxena, V. Srivastava, A. Kumar, *Eur. J. Med. Chem.* **2006**, *41*, 1223 – 1229.
[11] P. Singh, M. Kaur, P. Verma, *Bioorg. Med. Chem. Lett.* **2009**, *19*, 3054 – 3058.
[12] B. S. Jursic, F. Douelle, E. D. Stevens, *Tetrahedron* **2003**, *59*, 3427 – 3432.
[13] A. D. Brewer, J. A. Minatelli, J. Plowman, K. D. Paull, V. Narayanan, *Biochem. Pharmacol.* **1985**, *34*, 2047 – 2050.
[14] K. M. Khan, M. Ali, A. Ajaz, S. Perveen, M. I. Choudhary, *Lett. Drug Des. Discovery* **2008**, *5*, 286 – 291.
[15] B. S. Jursic, D. M. Neumann, *Tetrahedron Lett.* **2001**, *42*, 4103 – 4107.
[16] J. Wang, C. Medina, M. W. Radomski, J. F. Gilmer, *Bioorg. Med. Chem.* **2011**, *19*, 4985 – 4999.
[17] S. Rajamaki, A. Innitzer, C. Falciani, C. Tintori, F. Christ, M. Witvrouw, Z. Debyser, S. Massa, M. Botta, *Bioorg. Med. Chem. Lett.* **2009**, *19*, 3615 – 3618.
[18] J.-H. Lee, S. Lee, M. Y. Park, H. Myung, *Virol. J.* **2011**, *8*, 18.
[19] V. Balas, I. Verginadis, G. Geromichalos, N. Kourkoumelis, L. Male, M. Hursthouse, K. Repana, E. Yiannaki, K. Charalabopoulos, T. Bakas, *Eur. J. Med. Chem.* **2011**, *46*, 2835 – 2844.
[20] Z. Chen, D. Cai, D. Mou, Q. Yan, Y. Sun, W. Pan, Y. Wan, H. Song, W. Yi, *Bioorg. Med. Chem.* **2014**, *22*, 3279 – 3284.
[21] Q. Yan, R. Cao, W. Yi, L. Yu, Z. Chen, L. Ma, H. Song, *Bioorg. Med. Chem. Lett.* **2009**, *19*, 4055 – 4058.
[22] N. R. Penthala, P. R. Ponugoti, V. Kasam, P. A. Crooks, *Bioorg. Med. Chem. Lett.* **2013**, *23*, 1442 – 1446.
[23] H. M. Faidallah, K. A. Khan, *J. Fluorine Chem.* **2012**, *142*, 96 – 104.
[24] N. N. Pesyan, D. Soleimani, N. H. Jazani, *Turk. J. Chem.* **2015**, *39*, 998 – 1011.
[25] V. V. Dabholkar, D. T. Ravi, *J. Serb. Chem. Soc.* **2010**, *75*, 1033 – 1040.
[26] M. Kidwai, R. Thakur, R. Mohan, *Acta Chim. Slov.* **2005**, *52*, 88 – 92.
[27] Q. Yan, R. Cao, W. Yi, Z. Chen, H. Wen, L. Ma, H. Song, *Eur. J. Med. Chem.* **2009**, *44*, 4235 – 4243.
[28] Y. A. Elshaier, A. Barakat, B. M. Al-Qahtany, A. M. Al-Majid, M. H. Al-Agamy, *Molecules* **2016**, *21*, 1337.
[29] K. Padmini, M. Lohita, S. Sumakala, M. Vishnupriya, Y. Gowtham Kumar, E. Ramyasudha, *Asian J. Pharm. Anal. Med. Chem.* **2014**, *2*, 63 – 70.
[30] C. Hansch, S. M. Anderson, *J. Med. Chem.* **1967**, *10*, 745 – 753.
[31] J. T. Bojarski, J. L. Mokrosz, H. J. Bartoń, M. H. Paluchowska, *Adv. Heterocycl. Chem.* **1985**, *38*, 229 – 297.
[32] D. M. Neumann, A. Cammarata, G. Backes, G. E. Palmer, B. S. Jursic, *Bioorg. Med. Chem.* **2014**, *22*, 813 – 826.
[33] A. S. Al-Harbi, R. M. Abdel-Rahman, A. M. Asiri, *Int. J. Org. Chem.* **2014**, *4*, 142 – 153.
[34] B. S. Jursic, D. M. Neumann, *Tetrahedron Lett.* **2001**, *42*, 8435 – 8439.
[35] A. Sharma, Y. Jad, H. Ghabbour, B. de la Torre, H. Kruger, F. Albericio, A. El-Faham, *Crystals* **2017**, *7*, 31.
[36] A. Sharma, Y. Jad, M. R. Siddiqui, B. G. Torre, F. Albericio, A. El-Faham, *J. Chem.* **2017**, *2017*, 1 – 10.
[37] B. Coe, H. Grassam, J. Jeffery, S. Coles, M. Hursthouse, *J. Chem. Soc. Perkin Trans. 1* **1999**, 2483 – 2488.
[38] A. Basheer, Z. Rappoport, *J. Org. Chem.* **2006**, *71*, 9743 – 9750.
[39] R.-L. Meza-León, A. Dávila-García, F. Sartillo-Piscil, L. Quintero, M. S. Rivadeneyra, S. Cruz-Gregorio, *Tetrahedron Lett.* **2013**, *54*, 6852 – 6854.
[40] Clinical and Laboratory Standards Institute, *Performance Standards for Antimicrobial Susceptibility Testing, Sixteenth Informational Supplement*, **2006**, CLSI document M7 – A7, Clinical and Laboratory Standards Institute (CLSI), 940 West Valley Road, Suite 1400, Wayne, PA 19087-1898 (USA).
[41] L. Collins, S. G. Franzblau, *Antimicrob. Agents Chemother.* **1997**, *41*, 1004 – 1009.
[42] E. Esposito, R. Cortesi, M. Drechsler, L. Paccamiccio, P. Mariani, C. Contado, E. Stellin, E. Menegatti, F. Bonina, C. Puglia, *Pharm. Res.* **2005**, *22*, 2163 – 2173.

Manuscript received: June 20, 2018
Revised manuscript received: July 13, 2018
Accepted manuscript online: July 13, 2018
Version of record online: ■■ ■■, 0000

Antimicrobial analogue insight: Thiobarbituric acid (TBA) analogues with various functionalities at positions N and C5 were synthesized by acylation, Knoevenagel condensation, Schiff base, thioamide and enamine formation. They were then evaluated for antimicrobial activity, and Boc-protected amino acid conjugates at position C5 with an ethyl-substituted nitrogen atom were found to afford the best results; these could be useful in the design of future TBA-based derivatives.

A. Sharma, S. Noki, S. J. Zamisa, H. A. Hazzah, Z. M. Almarhoon, A. El-Faham, B. G. de la Torre,* F. Albericio**

■■ – ■■

Exploiting the Thiobarbituric Acid Scaffold for Antibacterial Activity

CHAPTER 3

Crystal Structure, Spectroscopic and Theoretical studies of Thiobarbituric Acid Derivatives: Understanding H-Bonding Pattern.

Anamika Sharma, Sizwe Zamisa, Sikabwe Noki, Zainab M.Almarhoon, Ayman El-Faham, Beatriz G.de la Torre and Fernando Albericio.

Published article

https://doi.org/10.1107/S2053229618015516

Acta Crystallographica Section C Peer-reviewed Journal.

Crystal Structures, Spectroscopic and Theoretical Studies of Thiobarbituric Acid Derivatives: Understanding H-Bonding Pattern

Authors

Anamika Sharma[a1], Sizwe Zamisa[b], Sikabwe Noki[b], Zainab M. Almarhoon[c], Ayman El-Faham[cd]*, Beatriz G. de la Torre[e]* and Fernando Albericio[bdfg]*

[a]School of Health Sciences, University of KwaZulu Natal, University Road, Westville, Durban, South Africa, 4000, South Africa

[b]School of Chemistry and Physics, University of KwaZulu Natal, Private Bag X54001, Westville campus, Durban, South Africa, 4000, South Africa

[c]Department of Chemistry, College of Science, King Saud University, 2455, Riyadh, Saudi Arabia, 11451, Saudi Arabia

[d]Department of Chemistry, Faculty of Science, Alexandria University, 426, Alexandria, Egypt, 21321, Egypt

[e]KRISP, College of Health Sciences, University of KwaZulu Natal, Durban, South Africa, 4001, South Africa

[f]Department of Organic Chemistry, University of Barcelona, Martí I Franqués 1-11, Barcelona, Spain, 08028, Spain

[g]CIBER-BBN, Networking Centre on Bioengineering, Biomaterials and Nanomedicine, Barcelona Science Park, Baldiri Reixac 10, Barcelona, Spain, 08028, Spain

Correspondence email: aymanel_faham@hotmail.com; garciadelatorreb@ukzn.ac.za; albericio@ukzn.ac.za

[1]Contributed equally
[2]Contributed equally

Funding information National Research Foundation (NRF) (Blue Sky's Research Programme # 110960) and the University of KwaZulu-Natal (South Africa); International Scientific Partnership Program ISPP at King Saud University (ISPP# 0061) (Saudi Arabia); Spanish Ministry of Economy, Industry and Competitiveness (MINECO) (CTQ2015-67870-P) and the Generalitat de Catalunya (2014 SGR 137) (Spain).

Abstract Owing to their wide application in pharmaceutical industry, thiobarbituric acid (TBA) derivatives are also known to possess applications in engineering and material sciences. 20 TBA derivatives with diversity at position "N" and at "C-5" through acylation, Schiff base formation, Knoevenagel condensation, thioamide, and enamine formation were studied. The absolute configuration for six derivatives was confirmed by single X-ray crystallography which indicates the formation of intramolecular H-bonding in all cases (**A01**, **A02**, **A06**, **A13**, **A17,** and **A18**) and also intermolecular H-bonding for **A17**. In **A13** presence of two intramolecular bonding was observed. The stabilization of enol over keto form was confirmed using Gaussian09 program package. In order to convert the keto form to the enol, an energy barrier of 55.05 kcal/mol needs to be overcome as confirmed by transition state calculations.

Keywords: Thiobarbituric acid; X-ray crystallography; UV spectroscopy; IR spectroscopy; DFT calculations; Transition state.

1. Introduction

A prerequisite for rational drug design and structure-based functional studies is the accurate knowledge about the molecular structure which is derived solely by X-ray crystallography (Aitipamula & Vangala, 2017, Deschamps, 2008, Zheng *et al.*, 2014). It is the most exhaustive technique available for determining 3-dimensional structure with correct configuration of the molecule at the atomic level. As structure and function are related, configuration plays a critical property in biological systems as changes in this may alter the response of the biologic system (Mason, 1983). Compounds containing BA/TBA moiety (**Figure 1**) plays a vital role as antianxiety agents in the central nervous system by binding to the γ-aminobutyric acid (GABA) receptor (Kapoor *et al.*, 2016, Ahluwalia & Aggarwal, 1996).

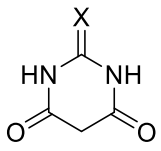

X = O Barbituric acid
X = S Thiobarbituric acid

Figure 1 The general structure of BA and TBA

Thiobarbituric acid (TBA) derivatives are widely used as privileged structures for a broad range of biological activity including antiepileptic, anticancer, antioxidant, anticonvulsant, immuno-modulatory, gelatinase inhibiting, HIV integrase inhibiting, antifungal, antiviral, tyrosinase inhibiting, anti-inflammatory and antidiabetic effects (Agarwal *et al.*, 2006, Singh *et al.*, 2009, Khan *et al.*, 2008, Jursic

& Neumann, 2001, Jursic *et al.*, 2003, Wang *et al.*, 2011, Rajamaki *et al.*, 2009, Lee *et al.*, 2011, Chen *et al.*, 2014, Penthala *et al.*, 2013). The bioactivity, however, differs from molecule to molecule depending on the tautomerization and the nature of the substituents (Chierotti *et al.*, 2010, Demeunynck *et al.*, 2006). Apart from its importance in the pharmaceutical industry, TBA derivatives are also known to possess, non linear properties (NLO), corrosion inhibition properties, application in analytical chemistry and are suitable for crystal engineering materials possessing specific, programmed properties due to their property of possessing both hydrogen bond donors and acceptors (Ivanova & Spiteller, 2010, Özcan *et al.*, 2008, Roux *et al.*, 2012).

Protons at position C-5 in TBA are highly acidic and hence undergo various reactions, including acylation and Knoevenagel condensation, among others (Faidallah & Khan, 2012). Substitution at C-5 increases lipophilicity and hence facilitates the transport of BA and TBA analogs towards their enzyme targets (Ahluwalia & Aggarwal, 1996). In view of the significance of TBA derivatives, we became interested in synthesizing new TBA derivatives with several C-5 substitutions including amino acids-TBA conjugates followed by DFT calculations to understand the keto-enol conformation of TBA derivatives.

2. Experimental

2.1. General

All reagents and solvents were purchased from commercial suppliers and were used without further purification unless otherwise stated. Fourier transform infrared spectroscopy (FTIR) spectra were recorded on Bruker-ALPHA Spectrophotometer in the spectral range 400-4000 cm^{-1}. The electronic spectra of the studied compounds (1 mg in 50 mL solvent) were measured using 3600 Series UV-Spectrophotometer in different solvents such as acetonitrile, ethanol, and dichloromethane. NMR spectra (^{1}H NMR and ^{13}C NMR) were recorded on a Bruker AVANCE III 400 MHz spectrometer. Chemical shift values are expressed in parts per million (ppm). Analytical HPLC was performed on Agilent 1100 system using Phenomena C_{18} column (3 µm, 4.6 × 50 mm), and Chemstation software was used for data processing over a 5-95 % gradient of CH_3CN (0.1% TFA)/ H_2O (0.1% TFA) over 15 min, flow rate: 1.0 mL/min, detection at 220 nm. High-resolution mass spectrometry (HRMS) was performed using a Bruker ESI-QTOF mass spectrometer in positive-ion mode.

2.2. Synthesis of derivatives

The derivatives (A01-A20) had been synthesized as reported by our group earlier (Sharma *et al.*, 2018). Further characterization:

5-acetyl-1,3-diethyl-2-thioxodihydropyrimidine-4,6(1H,5H)-dione (**A01**)

Pale white solid. 82% yield, mp = 40-42°C; HPLC t_R = 11.9 min; λ_{max} = 316 nm; IR (cm^{-1}): 1231 (C=S), 1685 (C=O); ^{1}H NMR (400 MHz, DMSOd_6): 1.18 (t, *J* = 7 Hz, -CH_3), 2.65 (s, -CH_3), 4.40 (q, *J* = 7 Hz, -CH_2); ^{13}C NMR (100 MHz, DMSOd_6): 11.8, 24.5, 42.5, 78.9, 97.4, 177.1, 197.3. HRMS: m/z: calcd. for $C_{10}H_{14}N_2O_3S$: 243.0798 $[M+H]^+$; found: 243.0811.

1,3-diethyl-5-propionyl-2-thioxodihydropyrimidine-4,6(1H,5H)-dione (**A02**)

Pale white solid. 56% yield, mp = 74-75°C; HPLC t_R = 12.9 min; IR (cm^{-1}): 1227 (C=S), 1680 (C=O); ^{1}H NMR (400 MHz, DMSOd_6): 1.14 (t, *J* = 7.4 Hz, -CH_3), 1.19 (t, *J* = 7.0 Hz, -CH_3), 3.11 (q, *J* = 7.4 Hz, -CH_2), 4.41 (q, *J* = 7.0 Hz, -CH_2); ^{13}C NMR (100 MHz, DMSOd_6): 8.9, 11.8, 30.7, 42.6, 96.6, 171.6, 177.0, 201.4. HRMS: m/z: calcd. for $C_{11}H_{16}N_2O_3S$: 257.0954 $[M+H]^+$; found: 257.0966.

5-benzoyl-1,3-diethyl-2-thioxodihydropyrimidine-4,6(1H,5H)-dione (**A03**)

Pale white solid. 36% yield, mp = 92-93°C; HPLC t_R = 13.1 min; IR (cm^{-1}): 1287 (C=S), 1675 (C=O); ^{1}H NMR (400 MHz, DMSOd_6): 1.18 (t, *J* = 7.0 Hz, -CH_3), 4.39 (q, *J* = 7.0 Hz, -CH_2), 7.4-7.6 (m, ArH); ^{13}C NMR (100 MHz, DMSOd_6): 12.1, 42.3, 96.3, 127.6, 128.4, 131.4, 137.1, 161.6, 167.3, 177.0, 192.3. HRMS: m/z: calcd. for $C_{11}H_{16}N_2O_3S$: 305.0954 $[M+H]^+$; found: 305.0957.

tert-butyl (1-(1,3-diethyl-4,6-dioxo-2-thioxohexahydropyrimidin-5-yl)-1-oxo-3-phenylpropan-2-yl)carbamate (**A04**)

Pale pink solid. 94% yield, mp = 130-131°C; HPLC t_R = 14.4 min; λ_{max} = 322 nm; IR (cm^{-1}): 1164 (C=S), 1682 (C=O) 3359 (N-H); ^{1}H NMR (400 MHz, DMSOd_6): 1.18 (t, *J* = 7.2 Hz, -CH_3), 1.28 (s, -CH_3), 3.09-3.12 (m, -CH_2), 4.44 (q, *J* = 7.2 Hz, -CH_2), 5.52 (t, J = 7.8, -CH), 7.16 (d, *J* = 7.3 Hz, -NH), 7.21-7.33 (m, ArH); ^{13}C NMR (100 MHz, DMSOd_6): 12.4, 18.8, 28.1, 45.7, 60.2, 69.9, 71.9, 125.7, 127.7, 129.3, 138.9, 155.1, 177.1, 183.8, 216.1. HRMS: m/z: calcd. for $C_{11}H_{16}N_2O_3S$: 448.1900 $[M+H]^+$; found: 448.1901.

1,3-diethyl-5-phenylalanyl-2-thioxodihydropyrimidine-4,6(1H,5H)-dione (**A05**)

Pale pink gum. 98% yield; HPLC t_R = 7.6 min; λ_{max} = 308 nm; ^{1}H NMR (400 MHz, DMSOd_6): 1.15 (t, *J* = 6.8 Hz, -CH_3), 3.08-3.12 (m, -CH_2), 4.20 (t, *J* = 5.5 Hz, -CH), 4.40 (q, *J* = 6.8 Hz, -CH_2), 7.23-7.30 (m, ArH), 7.72 (bs, -NH_2); ^{13}C NMR (100 MHz, DMSOd_6): 12.5, 41.5, 53.1, 58.5, 95.0, 128.4, 128.6, 129.4, 136.5, 160.2, 176.7, 189.6. HRMS: m/z: calcd. for $C_{11}H_{16}N_2O_3S$: 348.1376 $[M+H]^+$; found: 348.1388.

tert-butyl (1-(1,3-diethyl-4,6-dioxo-2-thioxohexahydropyrimidin-5-yl)-3-methyl-1-oxobutan-2-yl)carbamate (**A06**)

Dark pink solid. 92% yield, mp = 100-101°C; HPLC t_R = 14.1 min; λ_{max} = 320 nm; IR (cm^{-1}): 1105 (C=S), 1623 (C=O) 3369 (N-H); ^{1}H NMR (400 MHz, DMSOd_6): 0.81 (d, *J* = 6.8 Hz, -CH_3), 1.18 (t, *J* = 6.6 Hz, -CH_3), 1.37 (s, -CH_3), 3.06-3.11 (m, -CH), 3.80 (s, -CH), 4.41 (q, *J* = 6.8 Hz, -CH_2), 5.52 (d, *J* = 7.3 Hz, -CH), 6.87 (s, NH); ^{13}C NMR (100 MHz, DMSOd_6): 11.9, 28.1, 30.1, 42.6, 52.1, 58.9, 78.1, 139.1, 155.6, 168.7, 176.8, 199.5. HRMS: m/z: calcd. for $C_{11}H_{16}N_2O_3S$: 400.1901 $[M+H]^+$; found: 400.1884.

1,3-diethyl-2-thioxo-5-valyldihydropyrimidine-4,6(1H,5H)-dione (**A07**)

Dark pink gum. 97% yield; HPLC t_R = 6.6 min; ^{1}H NMR (400 MHz, DMSOd_6): 0.76 (d , *J* = 7 Hz, -CH_3), 1.2 (t, *J* = 7 Hz, -CH_3), 2.16 (m, -CH), 3.10 (m, -CH), 4.37 (q, *J* = 7 Hz, -CH_2), 4.96 (d, *J* = 8.5 Hz, -CH), 7.66 (bs, NH_2); ^{13}C NMR (100 MHz, DMSOd_6): 12.5, 15.8, 19.6, 29.1, 41.5, 61.5, 160.1, 176.7, 190.5. HRMS: m/z: calcd. for $C_{11}H_{16}N_2O_3S$: 300.1376 $[M+H]^+$; found: 300.1377.

(E)-1,3-diethyl-5-(1-((pyridin-2-ylmethyl)imino)ethyl)-2-thioxodihydropyrimidine-4,6(1H,5H)-dione (**A08**)

Pale yellow solid (gummy at room temperature). 86% yield; HPLC t_R = 8.8 min; ^{1}H NMR (400 MHz, $CDCl_3$): 1.22 (t, *J* = 7.0 Hz, -CH_3), 2.69 (s, -CH_3), 4.49 (q, *J* = 7.0 Hz, -CH_2), 4.75 (d, *J* = 5.6 Hz, -CH_2), 7.2-8.6 (m, ArH), 13.3 (s, -CH); ^{13}C NMR (100 MHz, $CDCl_3$): 11.4, 17.9, 41.8, 42.2, 48.2, 92.3, 120.4, 122.1, 136.3, 148.9, 153.3, 174.3, 176.6. HRMS: m/z: calcd. for $C_{11}H_{16}N_2O_3S$: 333.1380 $[M+H]^+$; found: 333.1387.

(E)-1,3-diethyl-5-(1-((4-methoxybenzyl)imino)ethyl)-2-thioxodihydropyrimidine-4,6(1H,5H)-dione (**A09**)

White solid. 69% yield, mp = 98-100°C; HPLC t_R = 12.6 min; ^{1}H NMR (400 MHz, $CDCl_3$): 1.21 (t, *J* = 6.9 Hz, -CH_3), 2.10 (s, -OCH_3), 2.66 (s, -CH_2), 3.75 (s, -CH_3), 4.47 (q, *J* = 7.0 Hz, -CH_2), 6.84-7.15 (m, ArH), 12.96 (s, -CH); ^{13}C NMR (100 MHz, $CDCl_3$): 11.4, 17.2, 41.8, 42.6, 46.8, 54.9, 113.7, 127.4, 130.1, 152.1, 154.4, 167.4, 173.6 HRMS: m/z: calcd. for $C_{11}H_{16}N_2O_3S$: 362.1533 $[M+H]^+$; found: 362.1535.

1,3-diethyl-5-(4-fluorobenzylidene)-2-thioxodihydropyrimidine-4,6(1H,5H)-dione (**A10**)

Yellow solid. 70% yield, mp = 180-182°C; HPLC t_R = 11.9 min; λ_{max} = 287 nm, 361 nm; IR (cm^{-1}): 1108 (C=S), 1614 (C=O); ^{1}H NMR (400 MHz, $CDCl_3$): 1.30 (t, *J* = 7.0 Hz, -CH_3), 4.59 (q, *J* = 7.0 Hz, -CH_2), 7.00-7.04 (m, Ar-H), 13.86 (s, -CH); ^{13}C NMR (100 MHz, $CDCl_3$): 12.1, 45.2, 97.4, 115.2, 115.4, 127.9, 128.0, 162.2, 163.7, 174.6. HRMS: m/z: calcd. for $C_{11}H_{16}N_2O_3S$: 307.0911 $[M+H]^+$; found: 307.0908.

5,5'-((3,5-dimethoxyphenyl)methylene)bis(1,3-diethyl-2-thioxodihydropyrimidine-4,6(1H,5H)-dione) (**A11**)

Yellow solid. 74% yield, mp = 150-151°C; HPLC t_R = 13.2 min; λ_{max} = 284 nm, 366 nm; ^{1}H NMR (400 MHz, DMSOd_6): 1.16 (t , J = 7.0 Hz, -CH_3), 3.44 (m, -CH), 3.62 (s, -OCH_3), 4.45 (q, J = 7.0 Hz, -CH_2), 6.10-6.26 (m, Ar-H), 8.10 (d, J = 6.6, -CH); ^{13}C NMR (100 MHz, DMSOd_6): 12.3, 18.5, 33.6, 42.8, 54.8, 96.3, 104.9, 145.2, 160.1, 161.1, 174.0. HRMS: m/z: calcd. for $C_{11}H_{16}N_2O_3S$: 549.1836 $[M+H]^+$; found: 549.1821.

5,5'-((2,4-dinitrophenyl)methylene)bis(1,3-diethyl-2-thioxodihydropyrimidine-4,6(1H,5H)-dione) (**A12**)

Buff solid. 76% yield, mp = 163-165°C; HPLC t_R = 12.2 min; λ_{max} = 289 nm; IR (cm^{-1}): 1108 (C=S), 1611 (C=O);^{1}H NMR (400 MHz, DMSOd_6): 1.14 (t , J = 6.7 Hz, -CH_3), 4.40 (q, J = 6.7 Hz, -CH_2), 6.42 (s, -CH), 7.51-8.41 (m, Ar-H); ^{13}C NMR (100 MHz, DMSOd_6): 12.1, 32.3, 42.8, 94.2, 118.9, 125.6, 130.9, 143.4, 145.5, 149.3, 160.7, 174.4. HRMS: m/z: calcd. for $C_{11}H_{16}N_2O_3S$: 579.1326 $[M+H]^+$; found: 579.1322.

1,3-diethyl-4,6-dioxo-2-thioxo-N-(p-tolyl)hexahydropyrimidine-5-carbothioamide (**A13**)

Pale yellow solid. 90% yield, mp = 132-133°C; HPLC t_R = 15.6 min; λ_{max} = 333 nm; IR (cm^{-1}): 1105 (C=S), 1645 (C=O);^{1}H NMR (400 MHz, DMSOd_6): 1.31 (t , J = 7.0 Hz, -CH_3), 2.39 (s, -CH_3), 4.58 (q, J = 7.0, -CH_2), 7.31-7.39 (m, Ar-H), 13.9 (s, -NH); ^{13}C NMR (100 MHz, DMSOd_6): 11.6, 20.7, 43.8, 91.7, 125.2, 129.5, 134.5, 137.0, 174.3, 184.9, 202.9. HRMS: m/z: calcd. for $C_{11}H_{16}N_2O_3S$: 350.0991 $[M+H]^+$; found: 350.0962.

2-thioxo-1,3-di-p-tolyldihydropyrimidine-4,6(1H,5H)-dione (**A14**)

Yellow solid. 92% yield, mp = 218-220°C; HPLC t_R = 10.2 min; λ_{max} = 241 nm, 286 nm; IR (cm^{-1}): 1339 (C=S), 1700 (C=O);^{1}H NMR (400 MHz, DMSOd_6): 2.27 (s, -CH_3), 7.12 (d, J = 8.1 Hz Ar-H), 7.33 (d, J = 8.1 Hz, Ar-H), 9.58 (s, -CH_2,); ^{13}C NMR (100 MHz, DMSOd_6): 21.1, 40.6, 128.4, 129.5, 136.6, 137.9, 169.3, 174.2. HRMS: m/z: calcd. for $C_{11}H_{16}N_2O_3S$: 325.1005 $[M+H]^+$; found: 325.1025.

5-acetyl-2-thioxo-1,3-di-p-tolyldihydropyrimidine-4,6(1H,5H)-dione (**A15**)

Yellow solid. 45% yield, mp = 185-186°C; HPLC t_R = 12.0 min; ^{1}H NMR (400 MHz, DMSOd_6): 2.34 (s, -CH_3), 2.65 (s, -CH_3), 7.15 (d, J = 8.2 Hz Ar-H), 7.26 (d, J = 8.2 Hz, Ar-H); ^{13}C NMR (100 MHz, DMSOd_6): 20.7, 24.5, 98.2, 128.5, 129.5, 136.7, 137.6, 179.6, 196.3, 206.9. HRMS: m/z: calcd. for $C_{11}H_{16}N_2O_3S$: 366.1077 $[M+H]^+$; found: 366.1100.

5-propionyl-2-thioxo-1,3-di-p-tolyldihydropyrimidine-4,6(1H,5H)-dione (**A16**)

Yellow solid. 57% yield, mp = 140-141°C; HPLC t_R = 12.7 min; λ_{max} = 318 nm; ^{1}H NMR (400 MHz, DMSOd_6): 1.14 (t, *J* = 7.4 Hz, -CH_3), 2.33 (s, -CH_3), 2.91 (q, *J* = 7.4 Hz, -CH_2), 7.08 (d, *J* = 8.2 Hz, Ar-H), 7.20 (d, *J* = 8.2 Hz, Ar-H); ^{13}C NMR (100 MHz, DMSOd_6): 10.1, 20.7, 30.1, 63.4, 128.5, 129.5, 137.6, 166.2, 170.6, 179.5, 187.6. HRMS: m/z: calcd. for $C_{11}H_{16}N_2O_3S$: 381.1290 $[M+H]^+$; found: 381.1267.

5-(1-aminoethylidene)-1,3-diethyl-2-thioxodihydropyrimidine-4,6(1H,5H)-dione (**A17**)

Yellow solid. mp = 190-191°C; HPLC t_R = 9.2 min; λ_{max} = 320 nm; IR (cm^{-1}): 1357 (C=S), 1613 (C=O) 3295 (N-H); ^{1}H NMR (400 MHz, DMSOd_6): 1.14 (t, *J* = 7 Hz, -CH_3), 2.53 (s, -CH_3), 4.37 (q, *J* = 7 Hz, -CH_2), 9.7 (s, -NH_2), 11.1 (s, -NH_2); ^{13}C NMR (100 MHz, DMSOd_6): 12.1, 24.3, 42.0, 91.2, 175.8, 176.9, 197.3. HRMS: m/z: calcd. for $C_{11}H_{16}N_2O_3S$: 242.0958 $[M+H]^+$; found: 242.0966.

5-(1-aminopropylidene)-1,3-diethyl-2-thioxodihydropyrimidine-4,6(1H,5H)-dione (**A18**)

Yellow solid. mp = 101-102°C; HPLC t_R = 10.1 min; ^{1}H NMR (400 MHz, DMSOd_6): 1.15 (t, *J* = 7.3 Hz, -CH_3), 1.16 (t, *J* = 6.9 Hz, -CH_3), 2.53 (q, J = 7.3 Hz, -CH_3), 4.40 (q, *J* = 6.9 Hz, -CH_2), 9.68 (s, -NH_2), 11.18 (s, -NH_2); ^{13}C NMR (100 MHz, DMSOd_6): 12.2, 12.7, 29.2, 42.1, 90.3, 161.2, 176.9, 180.6. HRMS: m/z: calcd. for $C_{11}H_{16}N_2O_3S$: 256.1080 $[M+H]^+$; found: 256.1096.

5-(1-aminoethylidene)-2-thioxo-1,3-di-p-tolyldihydropyrimidine-4,6(1H,5H)-dione (**A19**)

Yellow solid, mp = 198-200°C; HPLC t_R = 9.9 min; ^{1}H NMR (400 MHz, DMSOd_6): 1.23 (s, -CH_3), 2.33 (s, -CH_3), 7.07 (d, *J* = 8.2 Hz, Ar-H), 7.20 (d, *J* = 8.2 Hz, Ar-H), 9.69 (s, -NH_2), 10.9 (s, -NH_2); ^{13}C NMR (100 MHz, DMSOd_6): 20.8, 23.4, 101.2, 129.8, 132.4, 136.2, 137.3, 162.8, 167.3, 172.5. HRMS: m/z: calcd. for $C_{11}H_{16}N_2O_3S$: 366.1282 $[M+H]^+$; found: 366.1271.

5-(1-aminopropylidene)-2-thioxo-1,3-di-p-tolyldihydropyrimidine-4,6(1H,5H)-dione (**A20**)

Yellow solid, mp = 159-160°C; HPLC t_R = 10.6 min; ^{1}H NMR (400 MHz, DMSOd_6): 1.14 (t, *J* = 7.4 Hz, CH_3), 2.33 (s, -CH_3), 2.91 (q, *J* = 7.4 Hz, CH_2), 7.08 (d, *J* = 8.2 Hz, Ar-H), 7.20 (d, *J* = 8.2 Hz, Ar-H), 9.62 (s, -NH_2), 10.97 (s, -NH_2); ^{13}C NMR (100 MHz, DMSOd_6): 9.8, 20.7, 24.5, 98.2, 128.5, 129.5, 136.7, 137.6, 162.4, 179.6, 196.3. HRMS: m/z: calcd. for $C_{11}H_{16}N_2O_3S$: 380.1436 $[M+H]^+$; found: 380.1427.

2.3. Structure Determination

All non-hydrogen atoms were first refined isotropically and then anisotropically with full-matrix least squares based on F^2 using *SHELXL* (Sheldrick, 2015). All hydrogen atoms were positioned

geometrically, allowed to ride on their parent atoms, and refined isotropically. In A06, the hydrogen atom of the enol unit was found to be disordered over two positions between the enol and one of the carbonyl groups of the thiobarbituric ring. PART instructions were used to resolve the disorder and to achieve occupancy of 50% in the major component. Crystal data and structural refinement information are summarized in Table 2.

Table 1 Crystallographic data and structural refinement details of **A01**, **A02**, **A06**, **A13,** and **A18**.

	A01	**A02**	**A06**	**A13**	**A17**	**A18**
Chemical formula	$C_{10}H_{14}N_2O_3S$	$C_{11}H_{16}N_2O_3S$	$C_{18}H_{29}N_3O_5S$	$C_{16}H_{19}N_3O_2S_2$	$C_{10}H_{15}N_3O_2S$	$C_{11}H_{17}N_3O_2S$
M_r	242.29	256.32	399.50	349.46	241.31	255.33
Crystal system, space group	Monoclinic, $P2_1/n$	Monoclinic, $P2_1$	Orthorhombic, $P2_12_12_1$	Monoclinic, $P2_1/c$	Monoclinic, $P2_1/c$	Orthorhombic, $P2_12_12_1$
a, b, c (Å)	4.6212(1), 12.5742(4), 19.3936(6)	4.9140(1), 12.9450(3), 9.7630(3)	8.3816(12), 9.6258(14), 24.297(3)	4.8156(2), 21.7395(7), 15.1912(5)	12.8983(4), 9.8458(3), 18.2217(6)	4.9625(3), 10.6358(7), 23.2402(15)
α, β, γ (°)	90, 92.869(1), 90	90, 103.474(1), 90	90, 90, 90	90, 95.656(1), 90	90, 98.250(2), 90	90, 90, 90
V (Å^3)	1125.51(6)	603.95(3)	1960.3(5)	1582.61(10)	2290.10(13)	1226.62(14)
Z	4	2	4	4	8	4
μ (mm^{-1})	0.28	0.27	0.20	0.35	0.27	0.26
Crystal size (mm)	0.29 × 0.23 × 0.12	0.19 × 0.14 × 0.07	0.33 × 0.25 × 0.21	0.19 × 0.12 × 0.11	0.19 × 0.13 × 0.09	0.25 × 0.11 × 0.09
T_{min}, T_{max}	0.911, 0.978	0.940, 0.991	0.925, 0.968	0.925, 0.976	0.941, 0.985	0.924, 0.988
No. of measured, independent and observed [$I > 2\sigma(I)$] reflections	14896, 2704, 2309	8623, 2740, 2697	15347, 4505, 4245	25387, 4036, 3430	14727, 5036, 4323	10534, 2799, 2689
R_{int}	0.016	0.021	0.023	0.027	0.024	0.026
$(\sin\theta/\lambda)_{max}$ (Å^{-1})	0.667	0.650	0.654	0.675	0.642	0.649
$R[F^2 > 2\sigma(F^2)]$, $wR(F^2)$, S	0.030, 0.085, 1.05	0.024, 0.066, 1.08	0.029, 0.071, 1.04	0.031, 0.078, 1.04	0.033, 0.088, 1.03	0.029, 0.075, 1.06
Absolute structure parameter	—	0.035(16)*	0.00(2)*	—	—	-0.01(3)*

$\Delta\rho_{max}$, $\Delta\rho_{min}$ (e Å^{-3})	0.40, −0.19	0.25, −0.22	0.25, −0.18	0.38, −0.25	0.28, −0.27	0.31, −0.16

*Flack x determined using 1256, 1743, and 1059 quotients [(I+)-(I-)]/[(I+)+(I-)] for **A02**, **A06** and **A18**, respectively.

2.4. Theoretical Calculations

According to the above crystal structure, a crystal unit was selected as the initial structure, while DFT-B3LYP/6-311G++(d,p) methods in Gaussian09 (Frisch *et al.*, 2009) was used to optimize the structure of the title compound. No solvent corrections were made with these calculations. Vibration analysis showed that the optimized structure indeed represents a minimum on the potential energy surface (no negative eigenvalues). A four-membered ring transition state was calculated. The transition state was also confirmed using IRC (Gonzalez & Schlegel, 1989, 1990) calculations.

3. Result and Discussion

All the derivatives (Scheme 1) were synthesized earlier by our group (Sharma *et al.*, 2018) and well characterized by spectroscopic techniques which will be discussed in the subsequent sections.

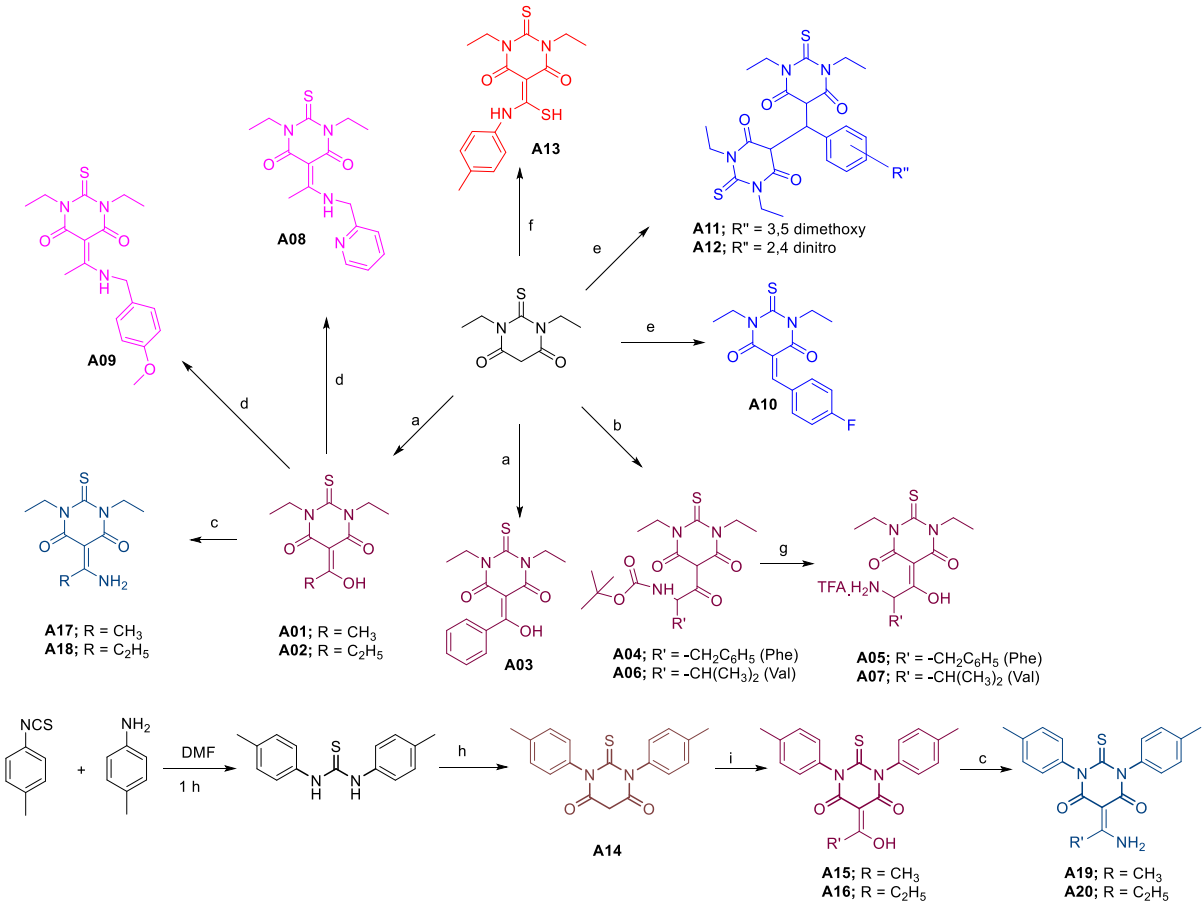

Scheme 1: a) Anhydride/$NaHCO_3$/H_2O, overnight; b) Boc-amino acid, EDC, HOBt, DMAP, DCM, 16 h; c) NH_4Cl/EtOH, overnight; d) Amine/Conc HCl/EtOH, overnight; e) aldehyde/EtOH, 10 min; f)

Isothiocyanate, DIEA, DCM, overnight; g) TFA, 1 h; h) malonic acid and acetyl chloride, 40 °C, 12 h; i) Acetic acid/Propionic acid, few drop conc H_2SO_4, reflux 1 h.

3.1. Synthesis and characterization

All the derivatives were synthesized earlier by our group (Sharma *et al.*, 2018) and were characterized by NMR followed by UV spectrometry using different solvents. Some of the derivatives (**A01**, **A02**, **A03**, **A04**, **A06**, **A10**, **A12**, **A13**, **A14,** and **A17**) were evaluated for IR spectroscopy and different absorption stretching frequencies were examined and compared with reported literature (Larkin, 2017). The absorption of thiocarbonyl (C=S) stretching frequency varies in three different ranges, 1395– 1570 cm^{-1}, 1260– 11420 cm^{-1} and 940 – 1140 cm^{-1} when attached with tertiary nitrogen and the absorption of C=S in all the spectra was found in range 1108-1357 cm^{-1} which is in agreement with reported literature (Pretsch *et al.*, 2000). In **A12** the absorption at 1377 cm^{-1} indicated the presence of a nitro group (NO_2). The presence of stretching frequency at 1680 cm^{-1}, 825 cm^{-1} and 1613 cm^{-1}, 838 cm^{-1} in **A01** and **A17** respectively, indicates the presence of "substituted alkene". A broad signal around 1541 cm^{-1} indicates the enol "-OH". A distinct signal at 3295 cm^{-1} in **A17** further indicates the presence of a primary amine, clearly confirming the enamine formation.

In **A01,** the C-5 proton in acetylated DETBA showed a signal at 17.72 ppm (singlet), which reflects the presence of OH, hence indicating that the enol form is more stable than the keto form. The enolization of the carbonyl group was also in excellent agreement with the observed 96.7 ppm for C-5 as shown by ^{13}C NMR. Furthermore, NMR for **A17**, **A18**, **A19,** and **A20** revealed the shift of peaks during the conversion from enol to enamine. Of note, we detected an interesting feature in all enamine derivatives where the "NH_2" proton showed two distinct peaks, one around 9.7 ppm and another at 11 ppm, clearly depicting different behavior of 2 protons in "-NH_2".

Given that the non-aromaticity of TBA, they absorb UV on the TLC plate and during the HPLC hence UV absorption of few derivatives was also studied using acetonitrile (ACN), ethanol and dichloromethane (DCM) as a solvent. 1,3-Diethyl-2-thiobarbituric acid (DETBA) showed λ_{max} absorption at 285 nm. **A01** showed absorption at a maximum (λ_{max}) of 316 nm, whereas **A04** and **A12** showed absorption at 322 nm and 289 nm respectively. However, similar results were obtained for **A12** in case of ethanol as a solvent but in case of DCM as solvent λ_{max} was observed at 305 nm. Also derivative with an aryl substitution on "N", **A14**, absorbed at 286 nm. However, with further substitution at C-5 in **A14** affording **A16**, shifts λ_{max} to 318 nm. Comparison of **A01** and **A17** revealed UV absorption changes from 316 nm to 320 nm as the conversion from keto to enamine form occurred.

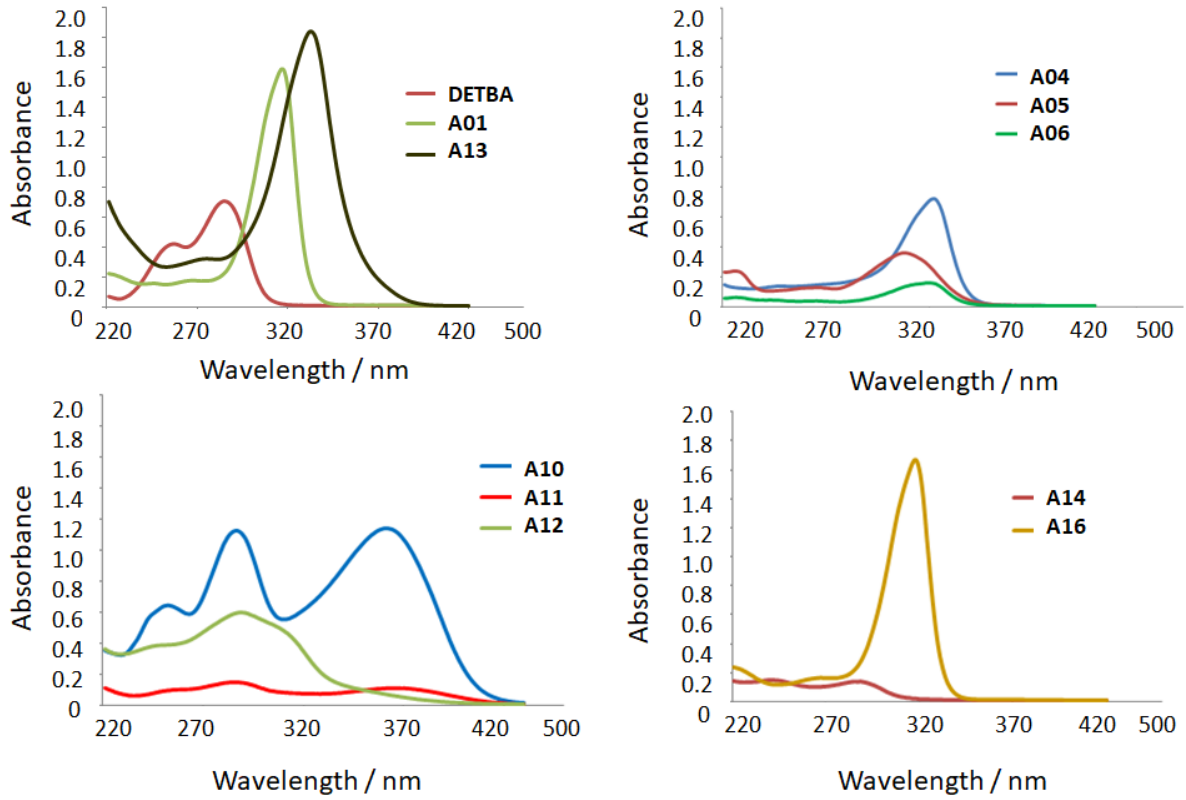

Figure 2 UV spectra of some TBA derivatives

In the case of **A04**, λ_{max} absorption was at 322 nm, and absorption shifted slightly to 308 nm after Boc removal in **A05**. **A06** showed λ_{max} absorption at 320 nm, a value that did not differ greatly from that of **A04**. UV-vis absorption was also studied for the Knoevenagel reaction (**A10** and **A11**). Two λ_{max} absorption peaks: one caused by DETBA and the other by the respective aldehyde were detected. For **A10**, λ_{max} absorption peaks were at 287 nm and 361 nm, whereas for **A11** they were at 284 nm and 366 nm. The reaction of DETBA with *p*-tolyl isothiocyanate resulted in **A13,** which has a thioamide bond which showed a shift from 285 nm (in case of DETBA) to 333 nm. Furthermore, **A14** showed two UV-vis absorption peaks at 241 nm and 286 nm, which were caused by the presence of "tolyl", as well as a "thiobarbituric ring".

3.2. Crystal structure descriptions of A01, A02, A06, A13, A17 and A18

Colorless X-ray quality crystals of **A01**, **A02**, **A06**, **A13**, **A17,** and **A18** were obtained by hot recrystallization from ethanol.

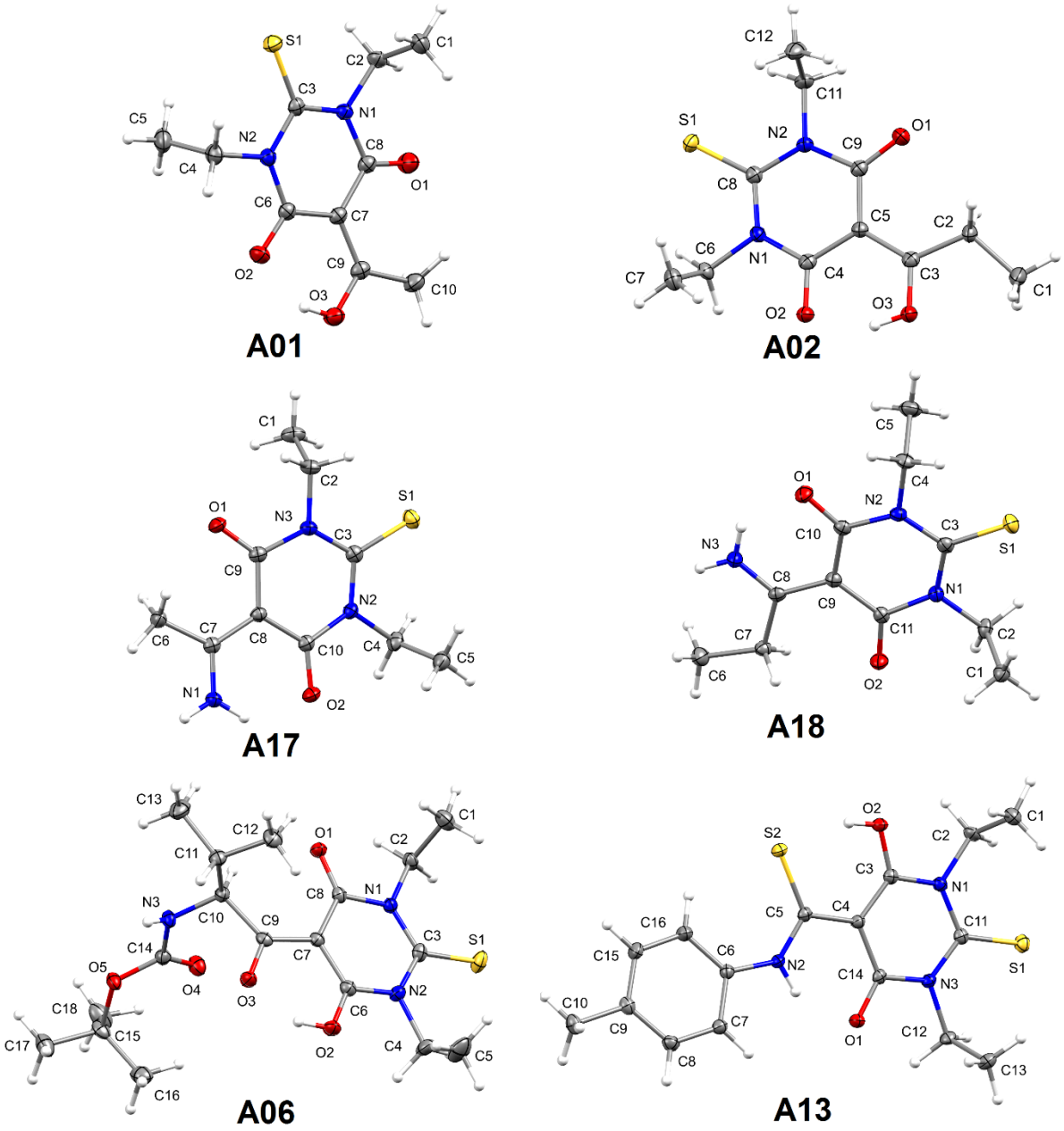

Figure 3 *ORTEP* diagrams of compounds **A01**, **A02**, **A06**, **A13**, **A17,** and **A18** drawn at 50% thermal ellipsoid probability. One of two molecules of compound **A17** was omitted for clarity.

Molecules in the asymmetric unit of these derivatives are shown in Figure 3. Each molecule consists of a DETBA ring with either an enol (in **A01**, **A02,** and **A06**), enamine (in **A17 A18**) or thioamide (in **A13**) moieties. The DETBA ring together with the various moieties was identified as planes that best describe the molecular conformations of **A01**, **A02**, **A06**, **A13**, **A17,** and **A18**. The DETBA, enol, enamine, and thioamide planes are denoted as P_{DETBA}, P_{ENOL}, P_{ENAMINE} and $P_{\mathrm{THIOAMIDE}}$, respectively, whilst the dihedral angles between corresponding planes are designated as P_{DETBA}—P_{ENOL}, P_{DETBA}—P_{ENAMINE} or P_{DETBA}—$P_{\mathrm{THIOAMIDE}}$. The dihedral angles between the various planes and root mean square deviation (RMSD) of fitted atoms of DETBA are listed in Table 2. The six-membered DETBA ring did

not appear to be completely planar in any of the compounds since the RMSD values of fitted atoms of DETBA rings were all greater than zero. The RMSD of P_{DETBA} increased as the carbon chain on the enol in **A01** (0.0187) extended to **A02** (0.0270). Interestingly, the presence of a bulky Boc-Val group to the enol in **A06** significantly improved the planarity of the P_{DETBA} over that observed in **A01**. However, the P_{DETBA}—P_{ENOL} dihedral angle appeared to increase with the carbon chain length and steric demand of the enol moiety. Compound **A17** is an enamine form of **A01** and showed RMSD values (0.0465—0.544) higher than those of all the enol counterparts with $\boldsymbol{P_{DETBA}}$—$\boldsymbol{P_{ENAMINE}}$ dihedral angles ranging between 5.2(2) and 7.9(2)°. In contrast to enol derivatives **A01** and **A02**, extending the carbon chain of the enamine forms of **A01** and **A02** led to a decrease in the RMSD of the DETBA ring from 0.0465—0.0544 (in **A17**) to 0.0245 (in **A18**). Exchanging the enamine for a thioamide moiety in **A13** resulted in the smallest dihedral angle (P_{DETBA}—$P_{THIOAMIDE}$ = 0.2(2)°) observed in this series, with a P_{DETBA} RMSD that was intermediate to that of the enol derivatives (Table 3).

Table 2 RMSD values of fitted atoms of P_{DETBA} and dihedral angles between P_{DETBA}—P_{ENOL}, P_{DETBA}—$P_{ENAMINE}$ and P_{DETBA}—$P_{THIOAMIDE}$ observed in **A01**, **A02**, **A06**, **A13**, **A17,** and **A18**.

Compound	RMSD of fitted atoms of $\boldsymbol{P_{DETBA}}$[a]	Dihedral angle [$\boldsymbol{P_{DETBA}}$—$\boldsymbol{P_{ENOL}}$[b]/$\boldsymbol{P_{ENAMINE}}$[c]/$\boldsymbol{P_{THIOAMIDE}}$[d]]/ °
A01	0.0187	6.3(1)
A02	0.0270	7.3(2)
A06	0.0117	8.7(2)
A13	0.0171	0.2(2)
A17	0.0544 0.0465	7.9(2) 5.3(2)
A18	0.0245	5.6(2)

[a]Atoms used t define P_{DETBA}: **(A01)** C3—C6—C7—C8—N1—N2; (**A02)** C4—C5—C9—N2—C8—N1; (**A06)** C8—C3—C6—N2—N1—C7; (**A13)** C3—C4—C11—C14—N1—N3; (**A17)** C3—C9—C10—C8—N3—N2; (**A18)** C3—C9—C10—C11—N1—N2
[b] Atoms used to define P_{ENOL}: (**A01**) C9—C10—O3; (**A02**) C1—C2—C3—O3; (**A06**) C9—C10—O3
[c] Atoms used to define $P_{ENAMINE}$: (**A17**) C6—C7—C8—N1; (**A18**) C6—C7—C8—N3
[d] Atoms used to define $P_{THIOAMIDE}$: (**A13**) C5—N2—S2

The bond distances and angles are comparable to related compounds (Coe *et al.*, 1999, Asiri *et al.*, 2009, Galán *et al.*, 2012, Bourhill *et al.*, 1994). However, bond parameters of interest in compounds **A01**, **A02**, **A06**, **A17,** and **A18** are summarized in Table 4. Compounds **A01** and **A02** displayed enolic properties, evidenced by a shorter $C_{carbonyl}$—$O_{carbonyl}$ (1.247(2)—1.257(2) Å) bond distance than C_{enol}—O_{enol} (1.309(2)—1.301(2) Å) which were comparable with that of the enamine forms, **A17** and **A18**. Furthermore, the $C_{ethylene}$—C_{enol} (1.398(2)—1.406(3) Å) appeared to be shorter than $C_{carbonyl}$—$C_{ethylene}$ (1.435(2)—1.430(3) Å). In compound A06, the $C_{carbonyl}$—$C_{ethylene}$ (1.404(2) Å) and C_{enol}—O_{enol} (1.260(2) Å) were significantly shorter than in **A01** and **A02**. This observation reveals electron

delocalization between a carbonyl group of the DETBA ring and the enol moiety, which is unique to **A06**.

Table 3 Selected bond parameters observed in **A01**, **A02**, **A06**, **A17,** and **A18**.

Bond parameter/Å	A01	A02	A06	A17	A18
$C_{carbonyl}$—$O_{carbonyl}$ [a]	1.247(2)	1.257(2)	1.250(2)	1.239(2) 1.237(2)	1.242(2)
$C_{carbonyl}$—$C_{ethylene}$ [b]	1.435(2)	1.430(3)	1.404(2)	1.434(2) 1.437(2)	1.436(3)
$C_{ethylene}$—$C_{enol/enamine}$ [c]	1.398(2)	1.406(3)	1.394(2)	1.425(2) 1.425(2)	1.430(3)
$C_{enol/enamine}$—$O_{enol}/N_{enamine}$ [d]	1.309(2)	1.301(2)	1.260(2)	1.308(2) 1.312(2)	1.314(2)

[a] (**A01**) C6—O2; **(A02**) C4—O2; (**A06**) C2—O6; **(A17**) C10—O2, C19—O4; (**A18**) C10—O1
[b] (**A01**) C6—C7; **(A02**) C4—C5; (**A06**) C6—C7; **(A17**) C10—C8, C19—C18; (**A18**) C10—C9
[c] (**A01**) C7—C8; **(A02**) C5—C3; (**A06**) C7—C9; **(A17**) C8—C7, C18—C17; (**A18**) C9—C8
[d] (**A01**) C9—O3; **(A02**) C3—O3; (**A06**) C9—O3; **(A17**) C7—N1, C17—N4; (**A18**) C8—N3

Hydrogen bonding patterns in the crystal packing of **A01**, **A02**, **A06**, **A13**, **A17,** and **A18** are shown in Figure 2, while the hydrogen bond parameters are listed in Table 4. Intramolecular O—H…O hydrogen bonds with graph-set notation $R_2^2(6)$ were observed in enol derivatives **A01**, **A02** and **A06**. Non-classical, intermolecular C—H…S hydrogen bonds linked neighboring molecules to form chains that a one-dimensional supramolecular structure that extended along the crystallographic *c* axis. In **A02**, intermolecular C—H…O hydrogen bonds joined adjacent molecules to form a two dimensional, honeycomb-like supramolecular network extending along the crystallographic *ab* axis. The N—H…S hydrogen bonds sewed together neighboring molecules of **A06** to form chains that extended along the crystallographic b axis. These chains were further joined via C—H…O hydrogen bonds along the crystallographic *a* axis to form a two-dimensional corrugated sheet-like supramolecular structure. A combination of intermolecular N—H…O and C—H…O hydrogen bonds (**A17**), formed six-membered rings with graphset notation $R_2^1(6)$ and resulted in a single-stranded helical supramolecular structure that elongated along the crystallographic *b* axis. On the other hand, N—H…O hydrongen bonds linked neighboring molecules to form chains that extended along the crystallographic *b* axis. Then C—H…O hydrogen bonds joined the chain along the crystallographic *a* anxis to form a two-dimensional, sheet-like supramolecular architecture.

3.3. Theoretical calculations

A density functional theory (DFT) geometry optimization with the Gaussian09 program package (Frisch *et al.*, 2009) employing the B3LYP (Becke three parameters Lee–Yang–Parr exchange-correlation functional, which combines the hybrid exchange functional of Becke (Becke, 1988) with the gradient-correlation functional of Lee, Yang and Parr (Lee *et al.*, 1988)) using 6-311G++(d,p) basis set was

performed in gas phase. No solvent corrections were made with these calculations as gas phase calculations frequently correspond quite well with crystal structures (Honarparvar *et al.*, 2013). Starting geometries for **A01**, **A04**, **A13**, **A17,** and **A18** were taken from X-ray refined data. The optimized geometry results in the free molecule state were compared to those in the crystalline state. No negative vibrational modes were obtained. The DFT calculated structure and geometric parameters (bond lengths and bond angles) were in agreement with each other. All optimized structures had a C1 point group.

The optimized geometry of **A01** indicates the electron delocalization between atoms C16-C17-C19-O28. The bond length between C19-O28 was 1.31 Å which is slightly higher than that of the carbonyl (C=O) (usually 1.22 Å), and H3-O3 formed a strong intra-molecular hydrogen bond with O2. However, **A04,** with a similar structure, showed delocalization of electrons in the TBA ring unlike that found in **A01** but also the presence of strong intra-molecular hydrogen bonding. **A13** showed the presence of two intra-molecular hydrogen bonds caused by the presence of a thioamide bond. **A17** and **A18** showed the presence of inter-molecular hydrogen bonding, in addition to intra-molecular hydrogen bonding.

3.3.1. Frontier Orbital Energy Analysis and Molecular Total Energies

Molecular Total Energy and Frontier Orbital energy levels were calculated using DFT (Table 5), as discussed previously by our group (Sharma *et al.*, 2017).

Table 4 Total energy and frontier orbital energy [B3LYP/6-311++G(d,p)] for **A01**.

--	**DFT (keto form)**	**DFT (enol form)**
E_{total}[a]	-1123.12965976	-1123.15077113
E_{HOMO}	-0.24121	-0.23291
E_{LUMO}	-0.09332	-0.09290
ΔE[b]	0.14789	0.14001

[a] 1 Hartree = 4.35974417 x 10^{-18} J = 27.2113845 eV; [b] $\Delta E = E_{LUMO} - E_{HOMO}$.

The crystal structure of **A01** (enol form) was used for DFT calculations. The energy gap between HOMO and LUMO was calculated by the B3LYP method using the 6-311G++(d,p) basis set. The title compound (in enol form) showed an energy gap (ΔE = 0.14001 Hartree = 3.78 eV) for HOMO $\rightarrow$ LUMO (Figure 4). This energy gap affords the theoretical absorption at λ_{max} = 326 nm. The keto form was optimized using GaussView05 (Dennington *et al.*, 2009), and the results were compared with those of the enol form (Table 4). The keto form showed an energy gap (ΔE = 0.14789 Hartree = 3.99 eV; λ_{max} = 308 nm) for HOMO $\rightarrow$ LUMO that was higher than that of enol form. HOMO and LUMO are important factors that affect bioactivity, chemical reactivity and electron affinity and ionization

potential (Clare, 1994, 1995, Zhang & Musgrave, 2007). Thus, the study of the frontier orbital energy can provide useful information about the biological and chemical reaction mechanism.

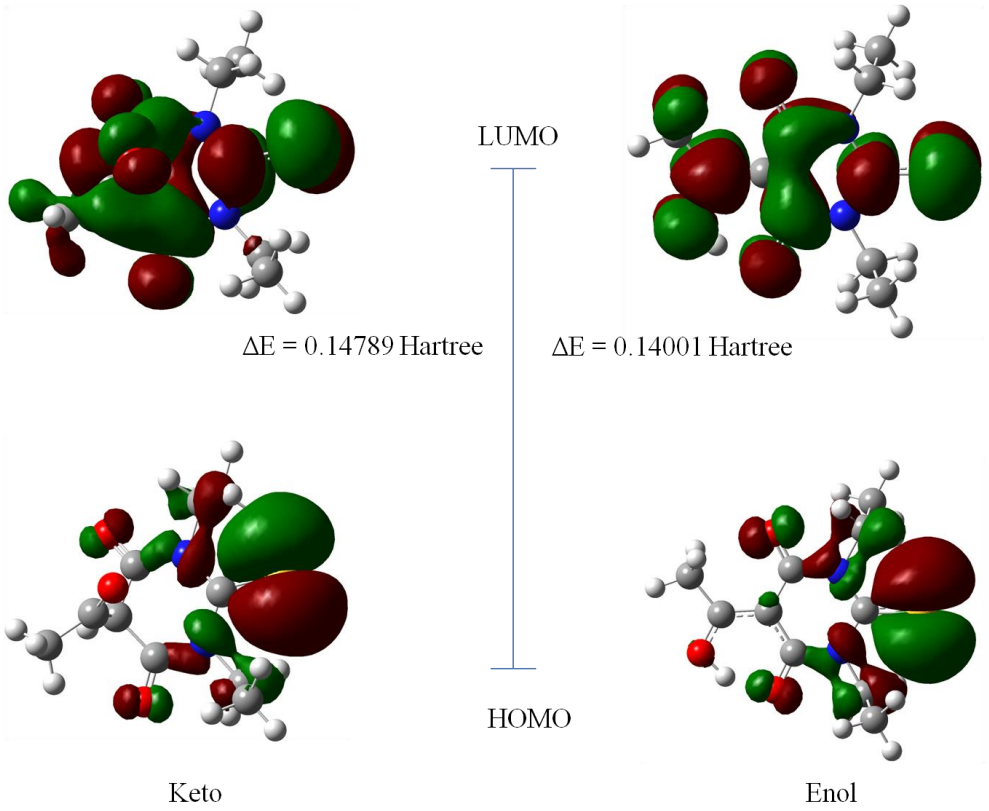

Figure 4 Frontier molecular orbitals of the title compound [B3LYP/6-311++G(d,p)].

3.4. Transition State Calculations

A transition state is broadly considered as the first order saddle point on the Potential Energy Surface (PES) of a molecular system. The vibrational spectrum of a transition state is characterized by one imaginary frequency (implying a negative force constant), which means that in one direction in nuclear configuration space the energy has a maximum, while in all other orthogonal directions the energy is a minimum (Lewars, 2003). In order to verify, **A01** (keto form) was optimized using Gaussian09, followed by frequency calculations at the same computational level as that used for the enol form (**A01**). The energies calculated are listed in Table 6 and shown schematically in Figure 5.

Table 5 Calculated reaction profile using DFT [B3LYP/6-311++G(d,p)].

--	**Relative Energies (kcal/mol)**
Keto form	0
Transition State	43.51
Enol form	-11.54

The calculated energy confirms that the reaction (Figure 5) is more favorable in a forward direction, i.e the enol form. In order to convert the keto form to the enol, an energy barrier of 55.05 kcal/mol needs to be overcome (Table 6); this value is much higher than the inherent energy limit of 15-20 kcal/mol at room temperature (Kruger, 2002, Singh *et al.*, 2012).

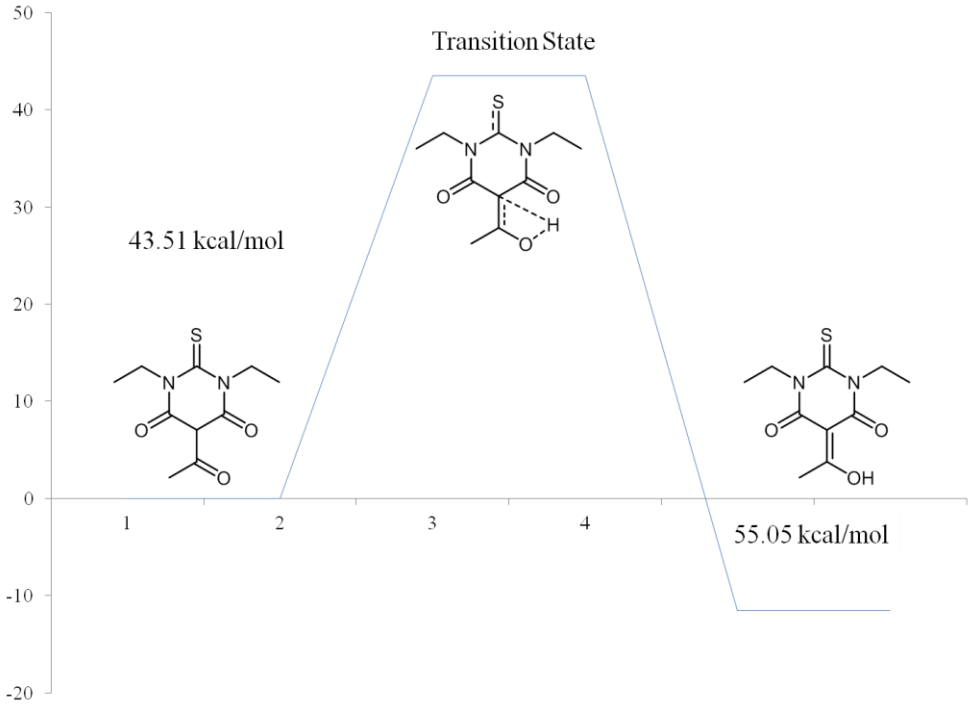

Figure 5 Transition state for a keto-enol form of **A01**.

The theoretical results thus suggest that if the product (enol) forms, it will not interconvert at room temperature. This notion was also confirmed by the NMR spectra (only the enol form was observed). A similar observation was made for all similar derivatives.

Conclusion

In conclusion, we have demonstrated the successful characterization of synthesized TBA derivatives by various spectroscopic techniques. The UV spectroscopy explained the absorptivity for the TBA derivatives at different wavelengths depending upon the structure. The λ_{max} for the TBA derivatives did not reveal any significant shift upon comparison with a change of solvent. The absolute configuration for six derivatives was confirmed by single ray X-ray crystallography which indicates the formation of intramolecular H-bonding in all cases (**A01**, **A02**, **A06**, **A13**, **A17,** and **A18**) and also intermolecular H-bonding for **A17**. In **A13** presence of two intramolecular bonding was observed. The acylation with simple carboxylic derivatives afforded the enamine, as shown by ^{1}H-NMR and X-ray crystallography. The stabilization of enol over keto form was confirmed using Gaussian09 program package. To convert the keto form to the enol, an energy barrier of 55.05 kcal/mol needs to be overcome as confirmed by transition state calculations. These studies provide an insight into the field of material

science since TBA derivatives possess good NLO properties and corrosion inhibition properties. These results also support the application of TBA derivatives in designing engineering material due to their property of possessing both hydrogen bond donors and acceptors.

References

Agarwal, A., Lata, S., Saxena, K., Srivastava, V. & Kumar, A. (2006). *Eur. J. Med. Chem.* **41**, 1223-1229.

Ahluwalia, V. & Aggarwal, R. (1996). *Proc. Indian Natl. Sci. Acad. Part A* **62**, 369-414.

Aitipamula, S. & Vangala, V. R. (2017). *J. Ind. Inst. Sci.* **97**, 227-243.

Asiri, A. M., Khan, S. A. & Ng, S. W. (2009). *Acta Crystallogr. Sect. E* **65**, o1820-o1820.

Becke, A. D. (1988). *Phys. Rev. A* **38**, 3098-3100.

Bourhill, G., Bredas, J.-L., Cheng, L.-T., Marder, S. R., Meyers, F., Perry, J. W. & Tiemann, B. G. (1994). *J. Am. Chem. Soc.* **116**, 2619-2620.

Chen, Z., Cai, D., Mou, D., Yan, Q., Sun, Y., Pan, W., Wan, Y., Song, H. & Yi, W. (2014). *Biorg. Med. Chem.* **22**, 3279-3284.

Chierotti, M. R., Ferrero, L., Garino, N., Gobetto, R., Pellegrino, L., Braga, D., Grepioni, F. & Maini, L. (2010). *Chem. Eur. J.* **16**, 4347-4358.

Clare, B. W. (1994). *Theor. Chem. Acc.* **87**, 415-430.

Clare, B. W. (1995). *Theochem* **331**, 63-78.

Coe, B., Grassam, H., Jeffery, J., Coles, S. & Hursthouse, M. (1999). *J. Chem. Soc., Perkin Trans. 1* **0**, 2483-2488.

Demeunynck, M., Bailly, C. & Wilson, W. D. (2006). *Small molecule DNA and RNA binders: from synthesis to nucleic acid complexes*. John Wiley & Sons.

Dennington, R., Keith, T. & Millam, J. (2009). *Semichem Inc., Shawnee Missions, KS.*

Deschamps, J. R. (2008). *Drug Addiction*, pp. 343-355: Springer.

Faidallah, H. M. & Khan, K. A. (2012). *J. Fluorine Chem.* **142**, 96-104.

Frisch, M. J., Trucks, G. W., Schlegel, H. B., Scuseria, G. E., Robb, M. A., Cheeseman, J. R., Scalmani, G., Barone, V., Mennucci, B., Petersson, G. A., Nakatsuji, H., Caricato, M., Li, X., Hratchian, H. P., Izmaylov, A. F., Bloino, J., Zheng, G., Sonnenberg, J. L., Hada, M., Ehara, M., Toyota, K., Fukuda, R., Hasegawa, J., Ishida, M., Nakajima, T., Honda, Y., Kitao, O., Nakai, H., Vreven, T., Montgomery Jr., J. A., Peralta, J. E., Ogliaro, F., Bearpark, M. J., Heyd, J., Brothers, E. N., Kudin, K. N., Staroverov, V. N., Kobayashi, R., Normand, J., Raghavachari, K., Rendell, A. P., Burant, J. C., Iyengar, S. S., Tomasi, J., Cossi, M., Rega, N., Millam, N. J., Klene, M., Knox, J. E., Cross, J. B., Bakken, V., Adamo, C., Jaramillo, J., Gomperts, R., Stratmann, R. E., Yazyev, O., Austin, A. J., Cammi, R., Pomelli, C., Ochterski, J. W., Martin, R. L., Morokuma, K., Zakrzewski, V. G., Voth, G. A., Salvador, P., Dannenberg, J. J., Dapprich, S., Daniels, A. D., Farkas, Ö., Foresman, J. B., Ortiz, J. V., Cioslowski, J. & Fox, D. J. (2009). *Gaussian 09.*

Galán, E., Andreu, R., Garín, J., Mosteo, L., Orduna, J., Villacampa, B. & Diosdado, B. E. (2012). *Tetrahedron* **68**, 6427-6437.

Gonzalez, C. & Schlegel, H. B. (1989). *The Journal of Chemical Physics* **90**, 2154-2161.

Gonzalez, C. & Schlegel, H. B. (1990). *Journal of Physical Chemistry* **94**, 5523-5527.

Honarparvar, B., Govender, T., Maguire, G. E., Soliman, M. E. & Kruger, H. G. (2013). *Chem. Rev.* **114**, 493-537.

Ivanova, B. & Spiteller, M. (2010). *Cryst. Growth Des.* **10**, 2470-2474.

Jursic, B. S., Douelle, F. & Stevens, E. D. (2003). *Tetrahedron* **59**, 3427-3432.

Jursic, B. S. & Neumann, D. M. (2001). *Tetrahedron Lett.* **42**, 8435-8439.
Kapoor, G., Pathak, D., Bhutani, P. & Kant, R. (2016). *J. Chem. Pharm. Res.* **8**, 151-168.
Khan, K. M., Ali, M., Ajaz, A., Perveen, S. & Choudhary, M. I. (2008). *Lett. Drug. Des. Discov.* **5**, 286-291.
Kruger, H. G. (2002). *Theochem* **577**, 281-285.
Larkin, P. (2017). *Infrared and Raman spectroscopy: principles and spectral interpretation*. Elsevier.
Lee, C., Yang, W. & Parr, R. G. (1988). *Phys. Rev. B* **37**, 785-789.
Lee, J.-H., Lee, S., Park, M. Y. & Myung, H. (2011). *Virol. J.* **8**, 1-4.
Lewars, E. (2003). *Computational Chemistry: Chapter 2- Introduction to the Theory and Applications of Molecular and Quantum Mechanics*, pp. 9-41. Boston, MA: Springer US.
Mason, S. F. (1983). *Trends Biochem. Sci* **8**, 422-423.
Özcan, M., Solmaz, R., Kardaş, G. & Dehri, I. (2008). *Colloids Surf. Physicochem. Eng. Aspects* **325**, 57-63.
Penthala, N. R., Ponugoti, P. R., Kasam, V. & Crooks, P. A. (2013). *Bioorg. Med. Chem. Lett.* **23**, 1442-1446.
Pretsch, E., Buehlmann, P., Affolter, C., Pretsch, E., Bhuhlmann, P. & Affolter, C. (2000). *Structure determination of organic compounds*. Springer.
Rajamaki, S., Innitzer, A., Falciani, C., Tintori, C., Christ, F., Witvrouw, M., Debyser, Z., Massa, S. & Botta, M. (2009). *Bioorg. Med. Chem. Lett.* **19**, 3615-3618.
Roux, M. V., Notario, R., Zaitsau, D. H., Emel'yanenko, V. N. & Verevkin, S. P. (2012). *J. Phys. Chem. A* **116**, 4639-4645.
Sharma, A., Jad, Y., Ghabbour, H., de la Torre, B., Kruger, H., Albericio, F. & El-Faham, A. (2017). *Crystals* **7**, 31.
Sharma, A., Sikabwe Noki, Sizwe J. Zamisa, Heba A. Hazzah, Ayman El-Faham, Beatriz G. de la Torre & Albericio, F. (2018). *ChemMedChem*, Manuscript Accepted.
Singh, P., Kaur, M. & Verma, P. (2009). *Bioorg. Med. Chem. Lett.* **19**, 3054-3058.
Singh, T., Kruger, H. G., Bisetty, K. & Power, T. D. (2012). *Comput. Theor. Chem.* **986**, 63-70.
Wang, J., Medina, C., Radomski, M. W. & Gilmer, J. F. (2011). *Biorg. Med. Chem.* **19**, 4985-4999.
Zhang, G. & Musgrave, C. B. (2007). *J. Phys. Chem. A* **111**, 1554-1561.
Zheng, H., Hou, J., Zimmerman, M. D., Wlodawer, A. & Minor, W. (2014). *Expert Opin. Drug. Discov.* **9**, 125-137.

CHAPTER 4

Conclusion

In conclusion, a series of thiobarbituric acid derivatives (**A01** to **A20**) were successful synthesized, using different techniques this include substitution at position "N" of structure with symmetrical substituents (**A14**, **A15**, and **A16**), and substitution at C-5 position this include acylation (**A01**, **A02**, **A03, A04, A05, A06,** and **A07**); Schiff base (**A08** and **A09**); Knoevenagel condensation (**A10**, **A11** and **A12**); Thioamide (**A13**) and enamine formation (**A17**, **A18**, **A19** and **A20**) . The antimicrobial test was performed against selected bacteria Gram +ve (*S.aureus* and *B.subtilus*) and Gram-ve (E. *coli* and *P. aeruginosa)* the results showed that the N-alkylated TBA derivatives and the acyl TBA derivatives have higher activity than the aromatic TBA derivatives ones; the TBA derivatives with the amino acid result showed that TBA derivatives with the Phe amino acid have higher activity than TBA derivatives with Val amino acid. In the case of cytoxicity, they are non-toxicity for the active TBA derivatives. (Chapter 2)

The characterization of TBA derivatives was successfully characterize with various spectroscopic techniques such as NMR, UV, IR, and X-ray crystallography. Here UV spectroscopy was used to identify the absorptivity of TBA derivatives at different wavelength since they are known non-aromatic compounds, the maximum wavelength of all derivatives was found in the range of 322 - 285 nm respectively. The crystal structures of six TBA derivatives (**A01**, **A02**, **A06**, **A13**, **A17,** and **A18**) were successfully evaluated and the configuration was confirmed by X-ray crystallography which indicates the formation of intramolecular H-bonding in all cases (**A01**, **A02**, **A06**, **A13**, **A17,** and **A18**) and also intermolecular H-bonding for **A17**. In **A13** presence of two intramolecular bonding was observed. The results of these TBA derivatives open up the possibility to explore more and construct new antibacterial agent using TBA moieties scaffolds, and their properties of possessing both hydrogen bond donors and acceptors put them in the position of being applicable in designing engineering material. (Chapter 3)

Supporting Information

In the CD, The characterization data of all synthesized TBA derivatives are attached,

This include:

- High-Performance Liquid Chromatography (HPLC)
- High-Resolution Mass Spectrometry (HRMS)
- Proton Nuclear Magnetic Resonance spectroscopy (^{1}H NMR)
- Carbon Nuclear Magnetic Resonance spectroscopy (^{13}C NMR)
- Infrared spectroscopy (IR)